CHARACTERIZATION OF A HYPERSPECTRAL IMAGER: A DIAGNOSTIC TOOL FOR MONITROING RETINAL DISEASES

by

NIRAD ZINZUWADIA

Presented to the Faculty of the Graduate School of

The University of Texas at Arlington in Partial Fulfillment

of the Requirements

for the Degree of

MASTER OF SCIENCE IN BIOMEDICAL ENGINEERING

THE UNIVERSITY OF TEXAS AT ARLINGTON

AUGUST 2007

ACKNOWLEDGEMENTS

I would like to take this opportunity to express my sincere gratitude to all those people who has helped me throughout the thesis work.

First, I would like to thank my supervisor and mentor Dr. Karel Zuzak, who provided me this opportunity to work on such an exciting project. He has always been there to encourage and support me in whatever I did. He has taught me, what research is and his guidance has helped me get better equipped to face challenges in my future endeavors. Thank you Dr. Zuzak.

I would also like to thank Dr. Doyle Hawkins, Associate Chair, Dept. of Mathematics for accepting to be a committee member and giving invaluable suggestion and statistical aid. I am grateful to Dr. Rafael Ufret-Vincenty, Assistant Professor, Dept. of Ophthalmology, UTSW for taking time from his schedule and being on my committee and for all your prompt replies.

I am grateful to Bhavesh Shah for his technical inputs and constant support during the project. I would also like to thank all of my lab mates for their ideas and suggestion.

Finally, I am greatly indebted to my parents, without whom this work would not have been possible. They have always inspired and encouraged me to achieve my goals.

July 20, 2007

ABSTRACT

CHARACTERIZATION OF A HYPERSPECTRAL IMAGER:

A DIAGNOSTIC TOOL FOR MONITROING

RETINAL DISEASES

Publication No. _____

Nirad Zinzuwadia, M.S.
The University of Texas at Arlington, 2007

Supervising Professor: Dr. Karel J Zuzak

We developed a novel hyperspectral slit lamp ophthalmoscope for visualizing vascular changes for clinical monitoring of retinal diseases, for example, diabetic retinopathy. The device consists of a visible charge couple device, CCD, and liquid crystal tunable filter, LCTF, coupled to the standard clinical slit lamp ophthalmoscope. The LCTF is used as a spectral light source illuminating the retina with different wavelengths of light that are recorded by the CCD and stored as a series of wavelength dependent images of the retina. Chemometric analysis produces a gray scale encoded image for the percentage of oxyhemoglobin at each pixel within the field of view. The system's spatial and spectral resolution and its wavelength tuning accuracy are characterized. The LCTF is continuously tunable in the spectral range of 520 – 602 nm

with a capability of passing light with a mean bandwidth of 9.60 nm. The system has a minimum spatial resolution of 0.11 mm when the retina is imaged at CCD binning of 4 X 4 and ophthalmoscope magnification of 10X. The overall acquisition time for the system is within 5 seconds. After characterizing the system, a proof of principle human retinal image is presented to demonstrate the capabilities of the system.

TABLE OF CONTENTS

LIST OF ILLUSTRATIONS

Figure Page

LIST OF TABLES

Table Page

CHAPTER 1

INTRODUCTION

1.1 Human Eye

The eye is an important and sensitive organ in the human body which allows us to visualize the world. The main function of human eye is photo-reception i.e. conversion of light energy to nerve action potential. These action potentials are subsequently relayed to the optic nerve and the brain, where further processing occurs, resulting in conscious vision [1].

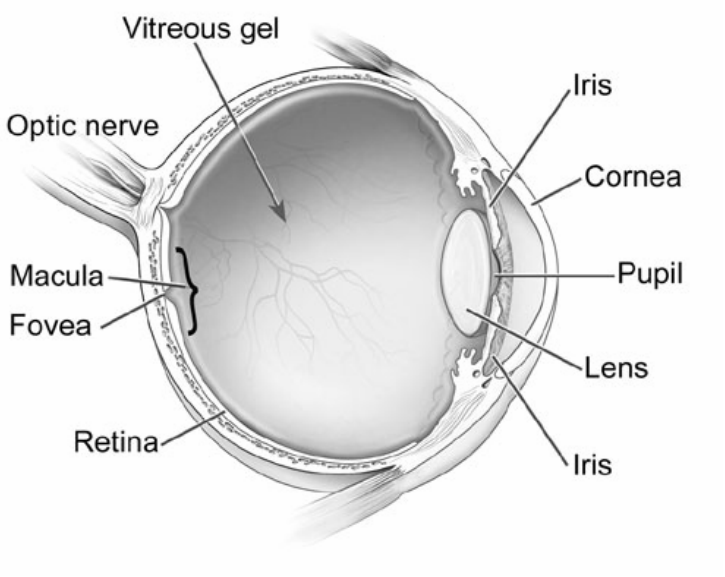

Figure 1: Cross sectional anatomy of the human eye [2]

Figure 1 shows the cross-sectional anatomy of the human eye along with its major structures. The light travels through cornea and lens and focuses on the retina. The conversion of photon to nerve impulses occur at retina before the final image is

generated. The cornea works as a secondary lens, focusing the incoming light onto the crystalline lens. It is responsible for 70 % of the total focusing of the eye. The iris is a thin diaphragm containing the pupil, which dilates and constricts and thus controls the amount of light that reaches the retina through the lens. The retina is the sensory tissue where the image is projected [3].

1.2 Why Retinal Imaging

Optical oximetry (spectroscopy) is widely used in clinical diagnostics and patient monitoring as it provides a non-invasive means of measuring hemoglobin saturation. Eye is the only organ where the arteries and veins are directly observable through the pupil. Because of this accessibility, investigators are prompted to apply optical oximetry for measurements of hemoglobin saturation at the fundus of the eye [4, 5].

Major application of this measurement (% HbO_2 and % Hb) is monitoring glaucoma, diabetic retinopathy and estimate blood loss in trauma victims non-invasively [5]. This measurement of hemoglobin saturation in retinal arteries and veins provides information regarding the oxygenation level in other important tissue. For instance, measurement of HbO_2 at retinal vessels provides an estimate of the cerebral hemoglobin saturation, since the blood supply to the retinal arteries originates via the ophthalmic artery from the internal carotid artery which supplies the cerebral tissue, Figure 2.

Various investigators have measured the retinal hemoglobin saturation using different algorithms. Hickam et. al. used two different wavelength combination in 1963. Hickam et. al. employed broadband Wratten filters centered at 640 nm and 800 nm using

a red-infrared instrument. This instrument was a fundus camera modified to take dual, quasi monochromatic retina photographs [5].

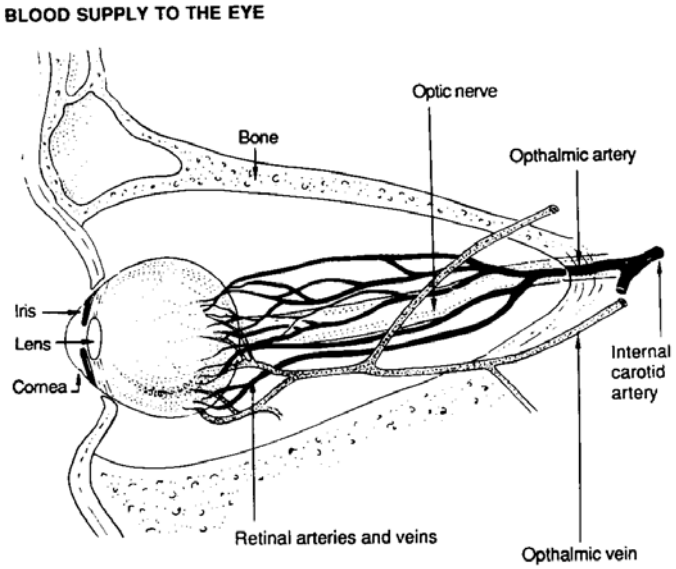

Figure 2: Schematic diagram showing the essential anatomy of the blood supply to the eye [6]

Delori in 1988 used three-wavelength retinal vessel oximeter for determining the oxyhemoglobin saturation. This device scanned a slit of filtered light across the retina and automatically processed the collected data. Delori used Pittman and Dulling method for estimating oxyhemoglobin saturation. There are other research groups who have made advancement, but providing accurate and reliable results remains an elusive goal [5].

This thesis work makes an attempt to measure the retinal oxy- and deoxy-hemoglobin saturation using a novel technique, hyperspectral imaging. We employ the slit lamp ophthalmoscope coupled with a CCD camera and a liquid crystal tunable filter to measure the hemoglobin saturation.

1.3 Blood Chromophore – Hemoglobin

Hemoglobin is a protein in the red blood cells that transports oxygen. It makes up about 97 % of the red cell's dry content and is produced in the bone marrow [7]. The hemoglobin molecule is made up of four polypeptide chains: two α chains, each with 141 amino acids and two β chains each with 146 amino acids. A heme is a flat ring molecule containing carbon, nitrogen and hydrogen atoms with a single iron ion at its center [8]. Heme is binding site for oxygen in hemoglobin. There are 4 heme groups in a hemoglobin molecule, each of which can bind one oxygen molecule, thus a hemoglobin molecule can bind 1 to 4 O_2 moleclues, ranging from the fully de-oxygenated to the fully oxygenated state [9].

Oxyhemoglobin is formed in lungs during respiration from where it travels to other organs of the body through circulatory system. Oxyhemoglobin has a specific absorption spectrum with absorption peaks at 540 nm and 576 nm in the visible spectrum. Deoxyhemoglobin has a different absorption spectrum with peak at 560 nm [10].

1.4 Hyperspectral Imaging

Hyperspectral imaging is a growing medical technology that combines and integrates spectral and spatial methods. Hyperspectral imaging acquires images over a spectral band of multiple wavelengths, generating precise optical spectral at each pixel in the data [11]. The data obtained is in form of a cube, referred as "image cube" having 2 spatial dimensions (X and Y) and 1 spectral dimension (wavelength, λ) [12]. A basic hyperspectral imaging system consists of a broad band light source, which, focuses the

light on the target, a sophisticated electronically tunable filter to spectrally discriminate large number of wavelengths with very narrow passband from the target, a charge couple device for collecting the spectrally discriminated light and convert them to a gray color-encoded image and a computer for data storage and analysis. The image acquisition process continues until all images at desired wavelength have been collected, generating the image cube [9]. An overview of Hyperspectral image cube is as shown in figure 3, A shows the sequence of images acquired simultaneously at different wavelength bands. The corresponding intensity values for a particular pixel taken along the series of image planes projected as a function of wavelength is depicted in B.

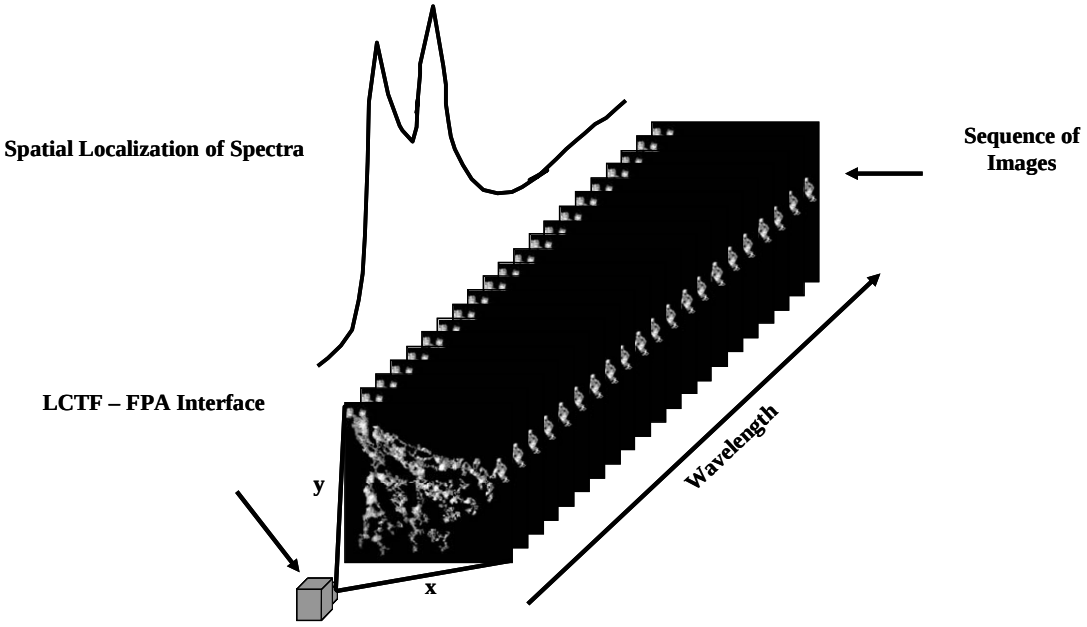

Figure 3: Hyperspectral Data Cube Visualization. A) Depicts sequence of images acquired at specific desired wavelengths. B) Depicts information obtained from each pixel within the hyperspectral image cube

Hyperspectral imaging could provide in vivo diagnosis of tissue without the need for biopsies in the case of cancer and early neoplastic changes. It has the capability of

early detection of retinal diseases as it provides information qualitatively (as is seen in the images) or quantitatively regarding vascular damage or decreased oxygen saturation [13] which can help in patient care as well.

Zuzak et. al. demonstrated the biomedical application of Hyperspectral Imaging technology at the National Institute of Health (NIH) to determine the percent oxyhemoglobin perfusing the skin tissue [14, 15]. Since then improvements have been made to the existing NIH prototype to develop both macroscopic and microscopic Hyperspectral Imaging system at UT-Arlington, which is used to determine the spectroscopy of different constituents present in the tissue. The microscopic system developed helps the ophthalmologists to visualize the retina and its associated structures thereby helping diagnosis and monitoring of various retinal diseases.

1.5 Research Problem

The primary goal of this thesis is to develop a prototype microscopic visible hyperspectral imaging system by modifying the existing multimodal microscopic hyperspectral imaging system, which will be capable of visualizing relative contribution of oxyhemoglobin in retinal tissue for clinical applications. Once the existing system is re-designed for retinal imaging, the system components comprising of CCD camera, LCTF and the ophthalmoscope will be calibrated. The next step will be imaging non-invasively the human retina to determine the distribution of oxyhemoglobin.

CHAPTER 2

METHOD

2.1 Instrument

The microscopic visible reflectance Hyperspectral imaging system shown here is modified and further enhanced in Laboratory of Biomedical Imaging at UTA for visualizing the retinal vasculature. This system can aid in early diagnosis and prognosis of various retinal diseases. The system is capable of providing the percentage of relative contribution of oxy- and de-oxyhemoglobin in the visible spectrum of light. The instrument was characterized and a proof of principle image of the retina was generated to measure the contribution of oxyhemoglobin in the blood vessels of the retina. The microscopic hyperspectral imager developed is depicted in figure 4.

The microscopic hyperspectral imager developed essentially consists of a slit lamp that illuminates the retina through the liquid crystal tunable filter. Thus instead of illuminating the target i.e. eye with a broad band of light, it is illuminated with different wavelengths of light in the visible region. This is unique about the system developed. Using LCTF as a spectral light source allows more light to be detected by the camera and allows less light shone to the retina. The slit lamp has built-in illumination system in form of halogen lamp. The light filtered by the liquid crystal tunable filter passes through the illumination optics above it and is focused onto the retina through the slit lamp aspheric lens. The light reflected from the retina and it's associated structure travels

back through the slit lamp aspheric lens and into the slit lamp microscope optics. The beam splitter within the ophthalmoscope splits the filtered light into two different path one of which focuses on the focal plane array and the second one, around 20 % of the intensity, to the eyepiece for the observer. The images formed at each wavelength on the focal plane array are then digitized and stored on the hard-drive for further analysis as wavelength dependent images.

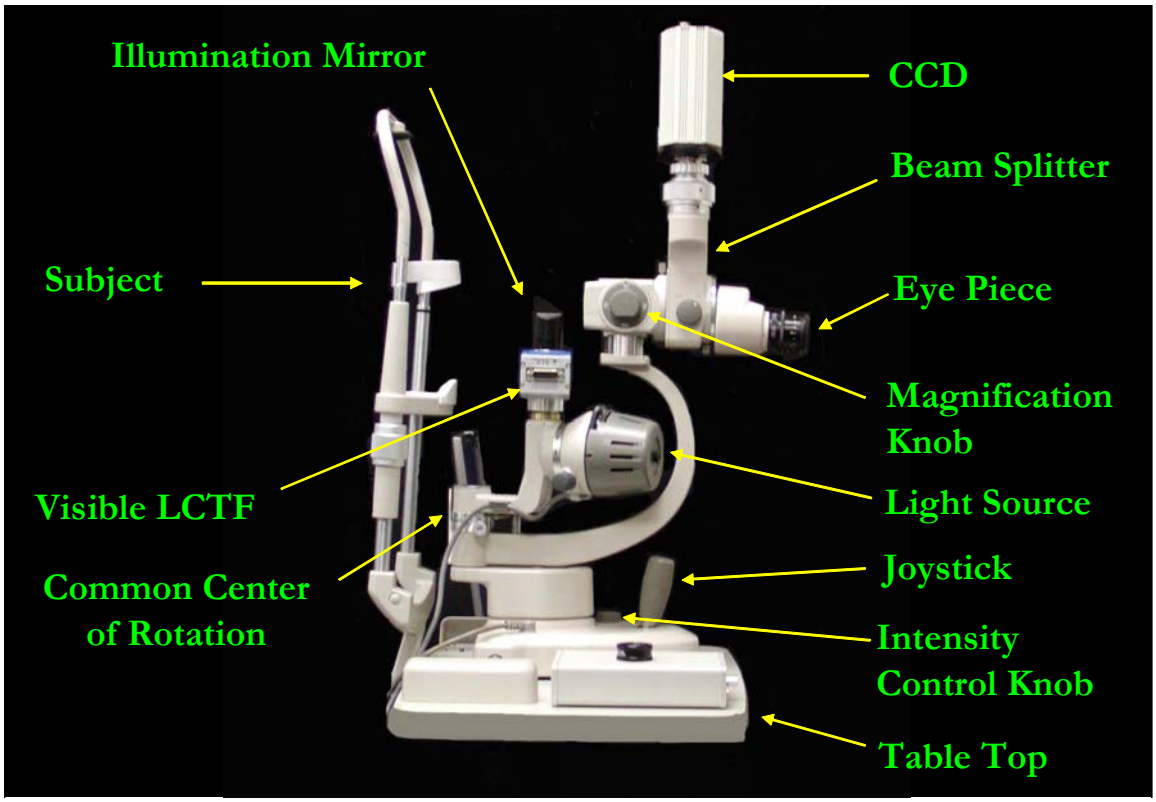

Figure 4: Visible Reflectance Hyperspectral Imaging System for visualizing retina

2.2 Slit Lamp

The slit lamp (Marco G2, Universal Ophthalmic Inc., Dallas, Texas) is the ophthalmologist's most frequently used and most universally applicable examination

instrument for eye [16]. The ophthalmoscope is essentially a microscope having two imaging lens (eyepiece and objective) and a condenser lens that provides optimum stereoscopic (3-D) observation with selectable magnification [16, 17]. The eyepiece and objective are responsible for magnifying the image of the specimen and projecting it onto the viewer's eye or onto the focal plane array. The word "slit lamp" originates from the fact that the illumination system is intended to produce a slit image that is as bright as possible, at defined distance from the instrument with its length, width and position being variable [17].

Figure 5: Marco G2 slit lamp

The Marco G2 slit lamp as shown in figure 5 has Galilean telescope for varying the magnification between 10x, 16x and 25x. The magnification knob on the slit lamp is highly maneurerable, allowing the operator to ajust power by feel without looking at the knob.

The microscope and the illumination system are mounted on a common vertical axis and can be moved independent of each other. In addition, the gear attached to the base of the ophthalmoscope provides fine precise movements of the microscope. These fine movements are controlled with the help of ergonomically designed joystick that has both lateral and vertical movements. The headrest accommodates most of the patient and the chin rest can be adjusted to get object in focus [18].

The illumination system consists of 12V / 30 W halogen lamp providing white broadband light. The optical light source embedded with the illumination system provides a clearer image. A compact transformer attached beneath the tabletop is used for generating the necessary voltage and wattage. A rheostat is also provided to get varying intensity of light and is located adjacent to the joystick for ease of use. In addition to the mechanical and illumination system, some of the other technical specifications are mentioned in the table 1 [18].

A beam splitter is used to partially transmit the light to the eye piece and rest to the CCD camera. It is essentially a half-silvered mirror and it placed between the microscope optics and the eye piece.

Table 1: Technical Specifications for the Marco G2 Slit Lamp Ophthalmoscope

Microscope	
Eyepiece	16x
Total Magnification	10x, 16x and 25x
Real Field of View	23 mm, 14 mm and 8.7 mm
Interpupillary Adjustment	47mm - 85mm
Slit Lamp	
Slit Projection	1x
Slit Width	0 - 14 mm
Slit Length	1 - 14 mm
Aperture Diaphragms	14 mm, 8 mm, 5 mm, 3 mm 0.3 mm
Filters	Heat absorbing, red-free & cobalt blue
Cross Slide Base	
Longitudinal Movement	90 mm
Lateral Movement	110 mm
Vertical Movement	± 15 mm
Horizontal Fine Movement	± 7.5 mm

2.3 Liquid Crystal Tunable Filter

The broad band white light from the slit lamp ophthalmoscope is filtered by the Liquid Crystal Tunable Filter, LCTF, (Cambridge Research & Instrumentation (CRi), Woburn, MA). LCTF behaves like interference filter with the difference being the wavelength range to be transmitted is electronically controlled, providing fast, accurate and vibration free selection of the wavelength [19]. The LCTF along with its control box is show in figure 6.

Figure 6: LCTF module comprising of LCTF and the control box [20]

Liquid-crystal tunable filter works on two principles: birefringence and polarization. It is essentially a multistage Lyot-Ohman type interference filter, but with a liquid crystal waveplate in each stage providing an electronically controllable variable retardance. A schematic of a single stage LCTF is shown in figure 7. The linearly polarized light passes through the birefringent element (fixed retarder), rotated 45^0 with respect to linear polarizer, where it experiences an optical path difference depending on the birefringence of the materials, the material thickness and the incident wavelength itself. [21, 22, 23].

After exiting through the fixed retarder, the light passes through the liquid crystal waveplate and finally through the linear polarizer. The last linear polarizer is oriented

parallel to the input linear polarizer. The electronically controlled waveplate is made up of combination of liquid crystal plate and a quartz plate, hence Liquid Crystal Tunable Filter. The liquid-crystal waveplate consists of two transparent electrodes (indium-tin oxide) on both sides of a cell containing liquid crystals that are initially aligned with their long axis nearly perpendicular to the light path.

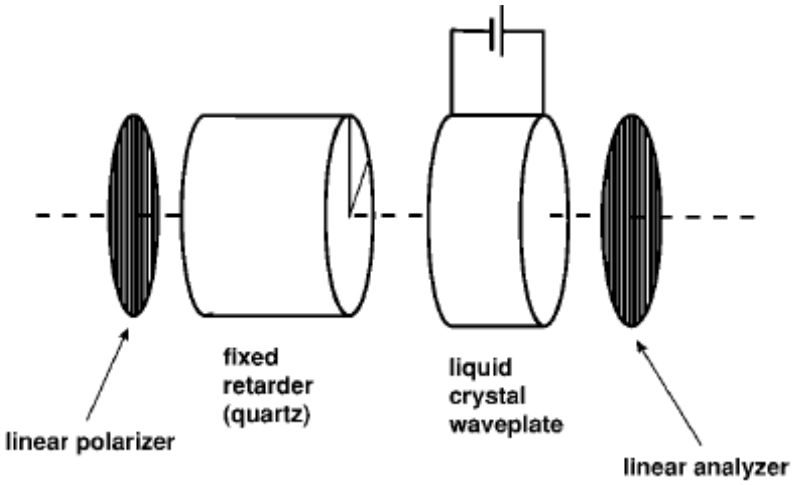

Figure 7: Schematic of a LCTF stage [23]

The inner surfaces of the cell are prepared in such a way that the molecules have a preferred orientation parallel to the surface. However, this orientation changes when an E-field parallel to the light path, twisting the direction of liquid crystal into the direction of the E-field. The twist of the liquid crystal in response to the E-field is proportional to the strength of the applied field. The resulting orientation of the molecules causes the retardance to change, producing a wavelplate with an electronically adjustable retardance [21, 22, 23]. Figure 8 shows the schematic representation of the liquid crystal in the presence of Electric field.

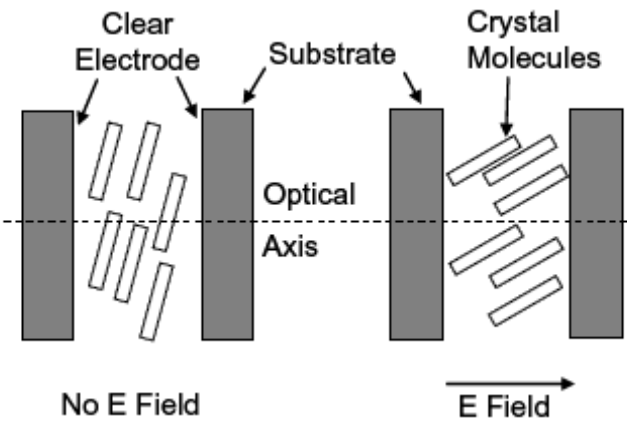

Figure 8: Schematic representation of alignment of liquid crystal in the presence of Electric field [24]

The light finally passes through the exiting linear polarizer, oriented parallel to incident linear polarizer and transmits wavelengths that have undergone an integral phase shift. To isolate a single wavelength λ, multiple retardance stages are needed. These subsequent stages are placed in series with retardance of each cell increased by a factor of 2. The transmittance through the LCTF is hence dependent on the integrated phase shift, which, in turn depends on the combined retardance. The polarizers between successive retarders offers better spectral control but the trade-off being transmittance through the LCTF. Each polarizer introduces a transmission loss of about 5 %, resulting in an overall transmission loss of 50 – 70 % [19 – 21], but if the light entering the incident polarizer is polarized, the transmission is increased by a factor of 2 as compared to randomly polarized light [20].

The spectral range of the LCTF is determined by the stage 1 of the filter which has the thinnest birefringent element and the bandpass is determined by the last stage which has the thickest element [23].

The LCTF module as shown in figure 6 consists of the filter (Optics Module) and the control box (Electronics Module). The module as a whole is very stable and provides accurate tuning of the wavelength independent of the ambient temperature in the range of 10^0 C to 40^0 C [20]. The host computer communicates through a hyper terminal and ASCII commands with the electronics module. The desired passband wavelength is fed to the electronics module, which calculates the required drive level (voltage) for each tunable element in the optics module [20, 25].

The response time, switching from one wavelength to another depends on various factors like liquid crystal relaxation time from "charge" to "no charge" state under various ambient temperatures and the calculation of the electronics controller box, which must send the correct voltages to each LC element for each change. Typically, response time is between 50 ms to 150 ms.

Some of the important specifications for the visible low resolution LCTF used in this project are tabulated in the table 2.

Table 2: Specifications for the visible low resolution LCTF

Parameters	**VariSpec VIS LCTF**
Clear Aperture	20 mm
Bandwidth (FWHM)	6 - 16 nm
Field of View (Half-Angle)	± 7.5^0 from normal
Wavelength range	400 - 720 nm
Wavelength accuracy	Bandwidth / 8
Optics response Time	50 ms
Operating Temperature	10^0 - 40^0 C

2.3.1 LCTF Operating Consideration

Some of the operating considerations for working of LCTF are discussed below.

2.3.1.1 Variation of FWHM with Pass Wavelength

The bandwidth is defined as full-width at half-maximum (FWHM) of the transmission curve i.e. in addition to the tuned wavelength, how many adjacent wavelengths are transmitted at FWHM. The FWHM is constant for Lyot filters and varies as 1/8 of the wavelength. The bandwidth is fixed for LCTF and cannot be adjusted in the field [25].

2.3.1.2 Response Time versus Tuning Wavelength

There is no simple relationship between the response time to change from one wavelength to another, and the wavelength involved, hence some wavelength requests tune more LC elements than other resulting in shorter or longer tuning speed [25].

2.3.1.3 Response Time versus Temperature

The liquid crystal variable retarders set the response time of the filter, and their viscosity varies with the temperature. High temperature (30^0 – 35^0 C) is preferable for LCTF working as it reduces the response time. If the optics temperature is cooler then 20^0 C, response time is longer than that given in the table 2 [25].

2.3.1.4 Thermal Drift and Re-Initialization

The filter exhibits slight drift when the optics module temperature changes resulting in a slight wavelength error, but performing the initialization routine renders the filter insensitive to temperature and reduces this error greatly. It the ambient temperature changes by more than ± 3^0 C, it is wise to re-initialize the filter [25].

2.4 Focal Plane Array (FPA)

The primary function of Charge Coupled Device (CCD) or FPA is to convert an incoming photon of light to an electron. In addition to charge generation, CCD accumulates and stores the charge, and transfers them when they are ready for read out. They can roughly be thought of as two-dimensional grid of individual photodiodes (pixels), each connected to its own charge storage "well". Each pixel senses the intensity of light falling on its collection area, and stores a proportional amount of charge in its associated "well". Once charge accumulates for the specified exposure time, controlled through software, the pixels are read out serially [26, 27].

The CoolSNAP$_{ES}$ manufactured by Princeton Instruments Inc. (formally Roper Scientific) is a scientific grade CCD used to acquire the hyperspectral data in the visible spectrum of light for retinal imaging. The major specifications for CoolSNAP$_{ES}$ are given in table 3.

The CoolSNAP$_{ES}$ monochrome camera, figure 9, incorporates a SONY ICX-285 silicon chip with Interline-transfer capability [9]. Interline-transfer CCD takes a structure such that the column of photo-sensing sites (so-called pixels) and vertical registers are arrayed alternately. The pixels convert the incoming light into electrical charge over a 1/60-sec period. After this period, the accumulated charges are transferred to the vertical shift registers during the vertical blanking period. The charges within the same line (the same row in the CCD array) are hen shifted down through the vertical shift register in the same sequence and read into the horizontal register, line-by-line [28]. The figure 10 shows the structure of Interline Transfer.

Table 3: Specifications for CoolSNAP$_{ES}$ camera

Specifications	
CCD Format	1392 x 1040 imaging array 6.45 x 6.45- µm pixels 8.77 x 6.6-mm imaging area (optically centered)
Well Capacity	16,000 e- (single pixel) 30,000 e- (2 x 2 binned pixel)
System Read Noise	< 8 e- rms @ 20 MHz
Nonlinearity	< 1 %
Dynamic Range	12 bits @ 20 MHz
Frame Readout	91 ms / frames
Cooling	Thermoelectric, 50 C below ambient temperature
Dark Current	1 e-/p/s
Operating Environment	15 ^{0}C to 30 ^{0}C ambient
Dimensions	4.5" x 5.0" x 2.5" (1.9 lbs)

Figure 9: CoolSNAP$_{ES}$ CCD Camera

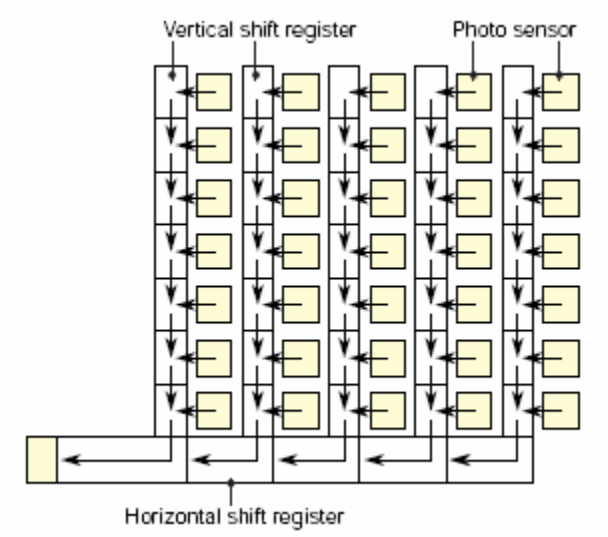

Figure 10: CCD Interline Transfer

The major drawback to interline transfer CCDs is poor sensitivity to photons since the opaque mask covers a large portion of each pixel [29]. To improve photon sensitivity, On-chip lens technology is used, that enhances light collecting capability. The microlens above each pixel effectively directs the light to them [28].

Another key feature of the SONY ICX-285 silicon ship is the anti-blooming capabilities. Blooming is migration of charges from one pixel to its adjacent pixel. The chip has the capability to remove the excess of charge generated from an overexposed pixel to the "drains", built within the CCD [28].

The electronic shuttering provided in this camera eliminates camera vibration and the ability to bin the camera increases signal to noise ratio while increasing the frame rate. The CoolSNAP$_{ES}$ has a digitizing speed of 20 MHZ and hence provides a high speed and high sensitivity readout over a high-resolution 1329 x 1040 imaging array [9].

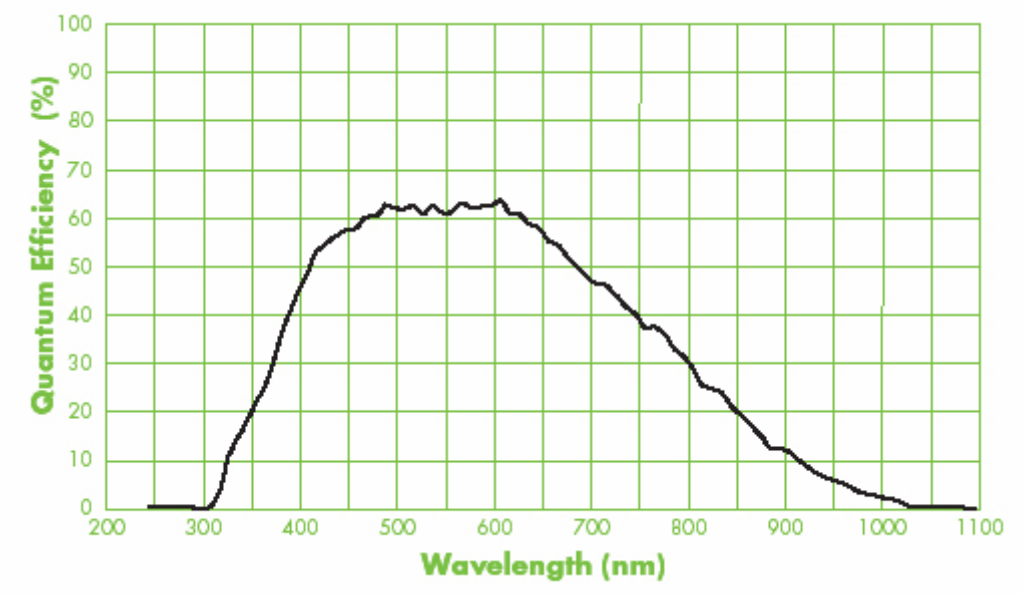

Figure 11: Spectral response of CoolSNAP$_{ES}$ CCD. Adopted from Photometrics Inc

The Quantum Efficiency (QE) of this camera is above 60 % in the region of interest i.e. between 500 – 650 nm and it is constant for this range of wavelengths. The spectral response for CoolSNAP$_{ES}$ is as shown in figure 11.

Apart from the characteristics mentioned above, CoolSNAP$_{ES}$ CCD has four different bin settings: 1 x 1, 2 x 2, 3 x 3 and 4 x 4. Higher bin setting reduces the exposure time for the experiment and requires less storage area with the trade-off being the spatial resolution. As the binning increases, the spatial resolution goes on decreasing. Technically, binning as shown in figure 12, is the process of adding the data from adjacent pixels together to form a single pixel (a super pixel), and binning can be accomplished either through hardware or software [9].

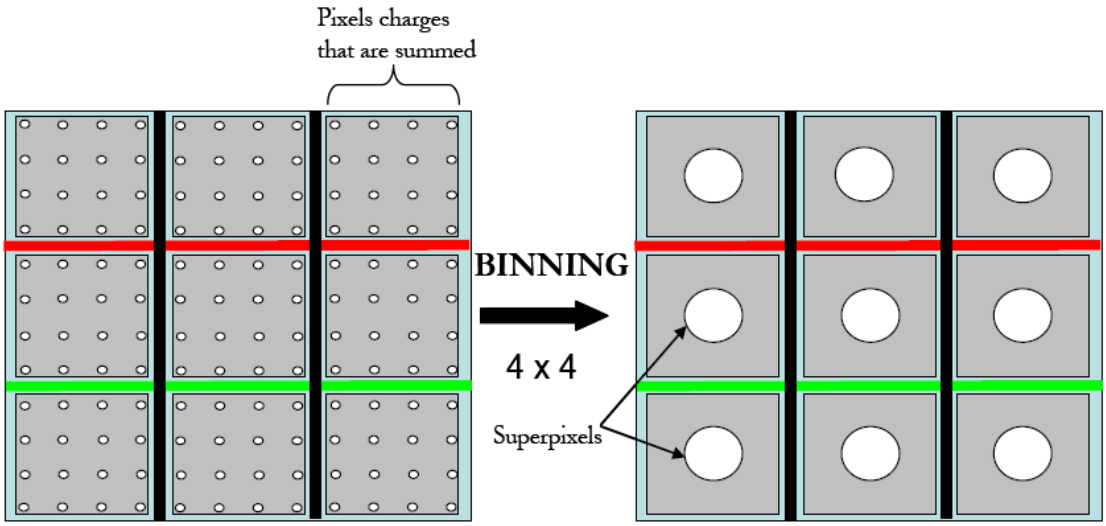

Figure 12: Formation of a single pixel from summation of 16 pixels, Hardware Binning 4 x 4 [9]

Hardware Binning is performed on the CCD array before the signal is read out of the output amplifier. Here adjacent pixels are transferred into the serial registers at a time and from there into the summing well. Finally, the pixels are summed up and showed a single pixel in final image. If the CCD has 12 μm pixels then 2 x 2 binning will yield an effective pixel size of 24 μm. Similarly, 3 x 3 binning will yield an effective pixel size of 36 μm and 48 μm if the binning is 4 x 4 [30].

One limitation of hardware binning is saturation, the point at which a pixel, the serial register or the summing well reaches its capacity. When saturation occurs any charge beyond the saturation value will be truncated and the final image will reflect the maximum pixel value rather than the actual value. The charge spilling also reduces the contrast [30]. The solution to this problem is software binning. However, software binning is not as fast as hardware binning.

CoolSNAP$_{ES}$ CCD is driven by PVCAM software, which stands for Photometrics Virtual Camera Access Method. PVCAM is a set of library routines that implements a camera's operation in a hardware-independent, platform-independent ("virtual") suite of function calls. The programming for setting up the experimental parameters like exposure time, binning, region of interest, and CCD gain, is done in Vpascal, which is integrated in V++. V++ is precision digital image processing and enhancement software and controls any PVCAM-compatible feature. The whole process of data acquisition is automated through V++ [31, 32].

2.5 Slit lamp aspheric Lens

The slit lamp ophthalmoscope doesn't allow direct viewing of the fundus of the eye. In order to have a better view of retinal blood vessels (part of fundus), the eye needs to be dilated through mydriatic eye drops, which dilates the pupil significantly and an aspheric diopter lens is needed to penetrate the light into the retina and get a hyperspectral image. We are using a 78D aspheric lens (Volk Optical Inc., Mentor, OH) for viewing the retina. The 78D aspheric lens is optimally designed for use within the range of motion of slit lamp [33]. The technical specification of aspheric diopter lens is mentioned in table 4 below. Figure 13 shows the side view of the 78D aspheric lens.

Table 4: Technical Specification for Volk 78D Aspheric Lens [33]

Lens	Field of View	Image Magnification	Working Distance
78D	81^0 / 97^0	0.93x	8 mm

Figure 13: Side view of Volk 78D aspheric slit lamp lens [33]

CHAPTER 3

EXPERIMENTAL SECTION

3.1 System Summary

The non-invasive, *in vivo*, microscopic visible reflectance Hyperspectral imaging system developed for retinal imaging is capable of generating a series of spectrally differentiated images using LCTF and CCD. In the conventional visible reflectance Hyperspectral imager, the broad band light source illuminates the target and the diffused reflected light is spectrally filtered through the LCTF and focused on the camera. In the system developed, LCTF is used as a spectral light source, where it filters the broad band light into individual wavelengths of light in the visible spectrum and then illuminating the retina. Finally, the reflected light falls on the detector, where it is converted to electrons, stored and read out at the end of single acquisition. The whole process of setting up of the experimental parameters, LCTF tuning, image acquisition and its storage in the hard-drive is automated through the computer program written in V++ and PVCAM, developed at National Institutes of Health. A personal computer (Dell Latitude D610) is employed for collecting and analyzing the data [14].

3.2 Reference Spectra

To calculate the relative contribution of HbO_2 and Hb for the Hyperspectral data using multi-variate least square analysis, reference spectra of HbO_2 and Hb are

required. Pure HbO_2 and Hb solutions were prepared at NIH by standard methods using blood collected from a healthy, non-smoking individual and reference spectra were obtained from the original system developed at NIH for the visible region (400 – 700 nm). A region of interest (520 – 645 nm) containing the peaks of oxy- and deoxy-hemoglobin was selected for imaging purpose in the visible region and the reference spectra for this region is shown in figure 14.

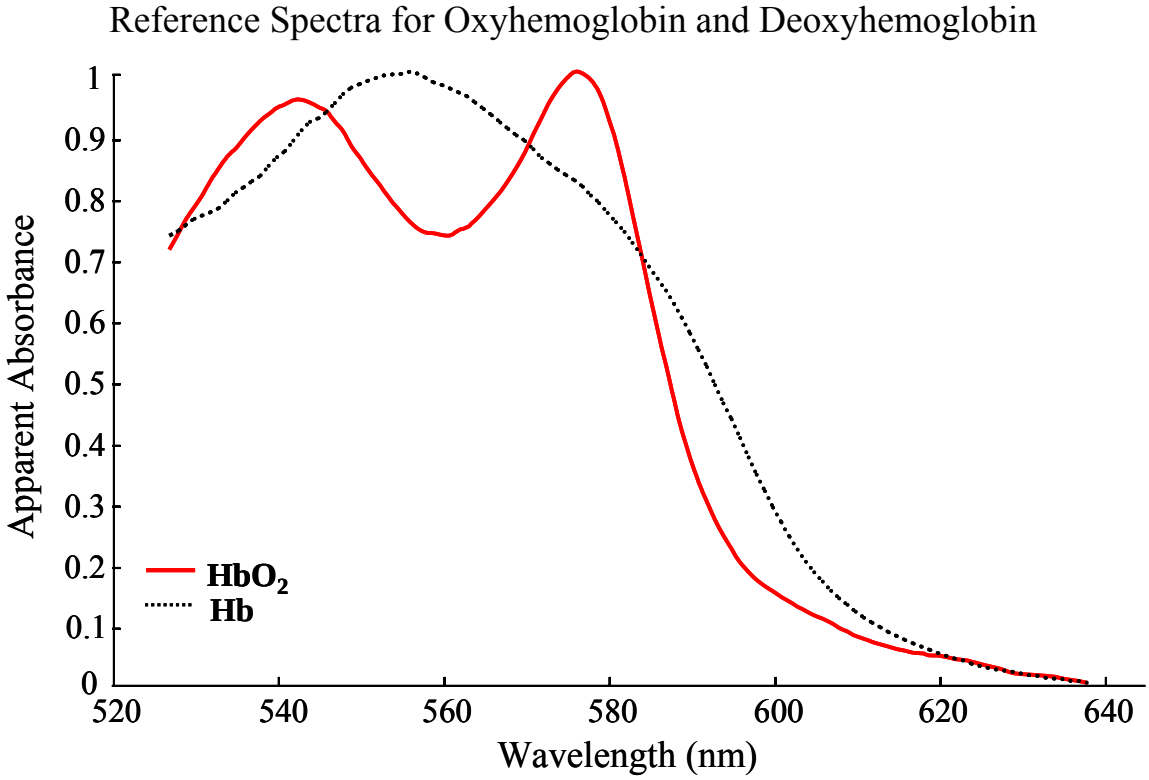

Figure 14: Reference Spectra for Oxyhemoglobin and Deoxyhemoglobin within visible region [15]

3.3 Experimental Protocol

A proof of principle clinical study was performed to demonstrate the functioning of the system as a tool for retinal imaging and measuring the relative contribution of

oxyhemoglobin in the retinal blood vessels. The data collection was done under the supervision of Dr. Karel Zuzak, Ph.D., in the Laboratory of Biomedical Imaging, UTA after receiving approval from The UTA Institutional Review Boards.

In this study, the retina was illuminated through the aspheric lens using the light source from the slit lamp for 5 seconds while acquiring the Hyperspectral image cube. The whole procedure is achieved in two steps: 1) Dilating the pupil and 2) Imaging the retina. When the subject entered the lab, the pupil was dilated through mydriatic eye drops (Cyclogyl, Alcon Lab, Fort Worth, TX). The subject relaxes for about 15 minutes, so as to dilate the pupils to its maximum. He was then asked to rest his chin onto the chinrest of the slit lamp. The aspheric lens was then placed near the eye and the eye piece was dragged to its end with the help of joystick. Slowly the eye piece was moved towards the eye along with maneuvering the diopter lens to get the retina in focus. Throughout the procedure, the subject was asked to keep his eyes steady and keep focus onto a particular point. Once in focus, the Hyperspectral image data cube was obtained within 5 seconds with aspheric lens in the light path.

3.4 Data Acquisition

The experimental setup for non-invasive, *in vivo,* microscopic Hyperspectral imaging system consisting of light source, LCTF, Beam splitter and the detector is shown in figure 15. The slit lamp having built in 12 V / 30 W halogen bulb providing a broad band light is used for imaging the retina. The broad band light is differentiated into individual band passes of wavelength through the LCTF in the visible region and

illuminates the target i.e. retina. The aspheric slit lamp lens and the microscope optics guides the reflected light onto the beam splitter, from where it is partially transmitted to the eye piece and rest to the detector, which directly sits on the C-mount of the ophthalmoscope. Integration of LCTF in light path to the target changed the height of the illumination mirror. To compensate for increase in height, a circular ring of 1" in length had be placed to raise the height of the microscope optics. This part was machined here in UTA workshop.

EXPERIMETNAL SETUP FOR HYPERSPECTRAL IMAGER

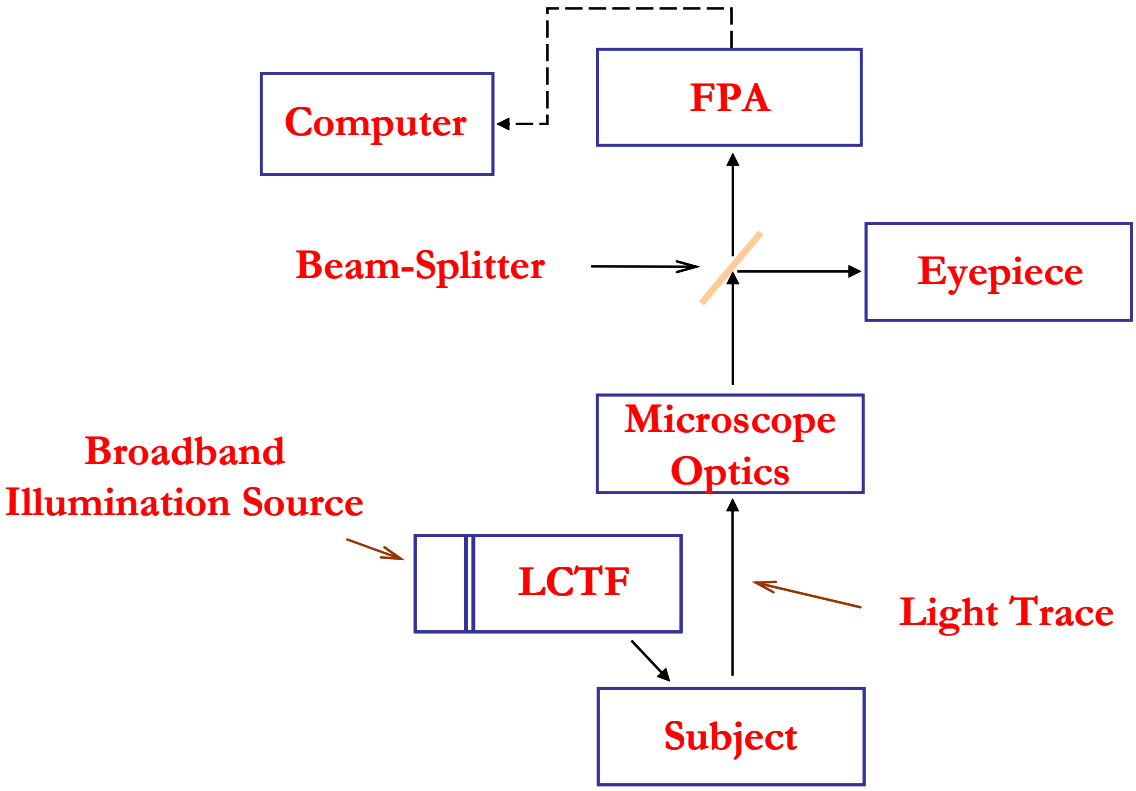

Figure 15: Experimental setup for imaging retina

The photons striking the FPA are digitized and transferred to a personal computer for post-processing. As mentioned earlier, the whole process of data acquisition right

from start till end is automated through the GUI built in V++. Before the start of the acquisition, the LCTF is initialized and the range of wavelength to be spectrally imaged is stored in control palette within the electronics module of LCTF in form of voltages. Initially the LCTF tunes to the first wavelength and image is acquired at the end of the preset exposure time (length of time that the CCD is accumulating charge in), transferred to the personal computer, and stored in form of a data file. The LCTF goes on tuning to each new wavelength and images are acquired and stored until all the wavelengths of interest are spectrally imaged.

The raw Hyperspectral data cube was collected using the CoolSNAP$_{ES}$ FPA, the low resolution LCTF scanned over a spectral range of 520 – 602 nm with a spectral increments of 2nm, the slit lamp microscope magnification of 10X and CCD binning of 4 x 4. The f / stop on the C-mount of the ophthalmoscope was adjusted to prevent saturation of pixels. The entire image was acquired within 5 seconds and stored to the hard-drive.

The V++ program automatically records the total time elapsed for one complete data acquisition. There are many factors, which affects the data acquisition time. The program first tunes the LCTF, which has an optical response time for tuning to a wavelength of interest. The optical response time is again dependent on ambient temperature; colder temperature causes the liquid crystal material to become more viscous and slower to respond. In addition to the optical response time, there is inherent tune wait time for each wavelength the LCTF tunes to i.e. time given to crystals in the optics module to settle for one particular passband. We usually set the tune wait time for

visible LCTF to 0 ms. The opening and closing of the camera shutter, though electronic also introduces some lag. Exposure time also affects the acquisition time. Higher exposure time yields longer acquisition period and vice-versa. Other factors that affects the total acquisition time are digitization time and time to bin the pixel. Since the CoolSNAP$_{ES}$ has a 20 MHz digitizer, the time required to convert data from analog format to digital format is quite small. The last factor affecting the acquisition time is the readout time, i.e. time required transferring the data from the CCD to the personal computer. Read out time is dependent on the clock speed of the processing unit, which in this case is 1.73 GHz. Summing up these times, the approximate time for acquiring one Hyperspectral data cube of 42 wavelengths and employing a binning of 4 x 4 turns out to be ~ 5 sec [34].

3.5 Determination of Experimental Parameters

High intensity light may be uncomfortable for the subject being examined and hence there are two competing issues in terms of light intensity that need to be balanced while acquiring a Hyperspectral image cube; keeping the intensity setting as low as possible to help with comfort, without affecting the brightness and spatial information of the final image. It is also important to acquire the image as quickly as possible using the lowest feasible exposure time. The data needs to be acquired quickly to reduce eye movement and hence the subsequent noise in the acquired images.

The macroscopic hyperspectral imager developed at NIH scanned the target over a spectral range of 520 – 645 nm with a spectral resolution of 1 nm over the range. This

range gives us 126 spectral images in one data cube. We selected the spectral range of 520 – 602 nm with an increment of 2 nm, giving 42 spectral images in single acquisition.

The first microscopic hyperspectral imaging system developed and characterized in Laboratory of Biomedical Imaging, UTA had LCTF placed in front of the detector instead of being used as spectral light source. This system was efficient for imaging the sclera of the eye and dermis of the skin [9], but suffered from inherent LCTF, relay optics and beam splitter limitation. The LCTF cuts nearly 60 – 80 % of the incoming light and there are some losses at beam splitter. As a result the system was not able to get sufficient photon count when retina was imaged, though retina was visible through the eye piece.

Since we cannot increase the intensity of the source to its maximum or have a long exposure time for CCD, we thought of changing the position of the LCTF and using it as spectral light source. Initially the LCTF was placed right in front of the halogen bulb. But this configuration did not offer any advantage. The halogen bulb gets heated up and this heat is transferred to the LCTF. The immediate effect is the increase in the LCTF temperature and it rapidly shoots above 40^0 C, which is not favorable for normal LCTF operating condition.

Secondly, we thought of placing the LCTF right beneath the illumination prism as shown in figure 4 and removing the small hollow tube between the lamp source and the illumination prism. This new position of LCTF required machining of the additional parts as mentioned above. In addition, we placed the camera directly onto the C-mount of the ophthalmoscope. This configuration had a couple of advantages: 1) the intensity of the slit lamp source now is not dependent on eye and can be varied to have a bright

illumination of retina, since the LCTF cuts significant amount of light. This fact is further elaborated in chapter 4 and 2) the counts can be increased significantly while keeping the exposure time as small as possible, as the reflected light from the retina now focuses directly on the CCD. This configuration speeds up the acquisition time significantly.

As mentioned above, setting the magnification to 10X and binning of 4 x 4, the exposure time for the CCD was calculated using the 99 % reflectance target. The exposure time for the CCD was set experimentally, by tuning the LCTF to 602 nm, having highest transmittance in the spectral range. The spectralon (Labsphere Inc., SRT-99-120, Sutton, NH) was then kept in the light path, since it has 99 % reflectance, giving us the highest intensity at 602 nm and relatively lower intensity count for rest of the wavelengths. The spectral output is as shown in figure 16. The spectral output depicts the response of LCTF and it is theoretically linear in this operating range. The exposure time was determined so as to have the highest count on the CCD to be around 3800 photons @ 602 nm.

3.6 Data Analysis

The hyperspectral data cube was analyzed to quantitatively determine the relative percent contribution of oxyhemoglobin and deoxyhemoglobin over the region of interest. Matlab (The Mathwork, Natick, MA) was used for writing the specific code for processing and analyzing the data.

Determining the percentage of HbO_2 is a two-fold process. First, the measured visible reflectance spectra are quantified in terms of apparent absorbance, $A_{xy}(\lambda_i)$, a ratio

between the reflected sample radiation, $R_{xy}(\lambda_i)$, and the reflected radiation from a spectralon (99.9 % reflective target), $R_{xy}(\lambda_i)_o$, measured at wavelength λ_i for the spatial coordinates x and y [14].

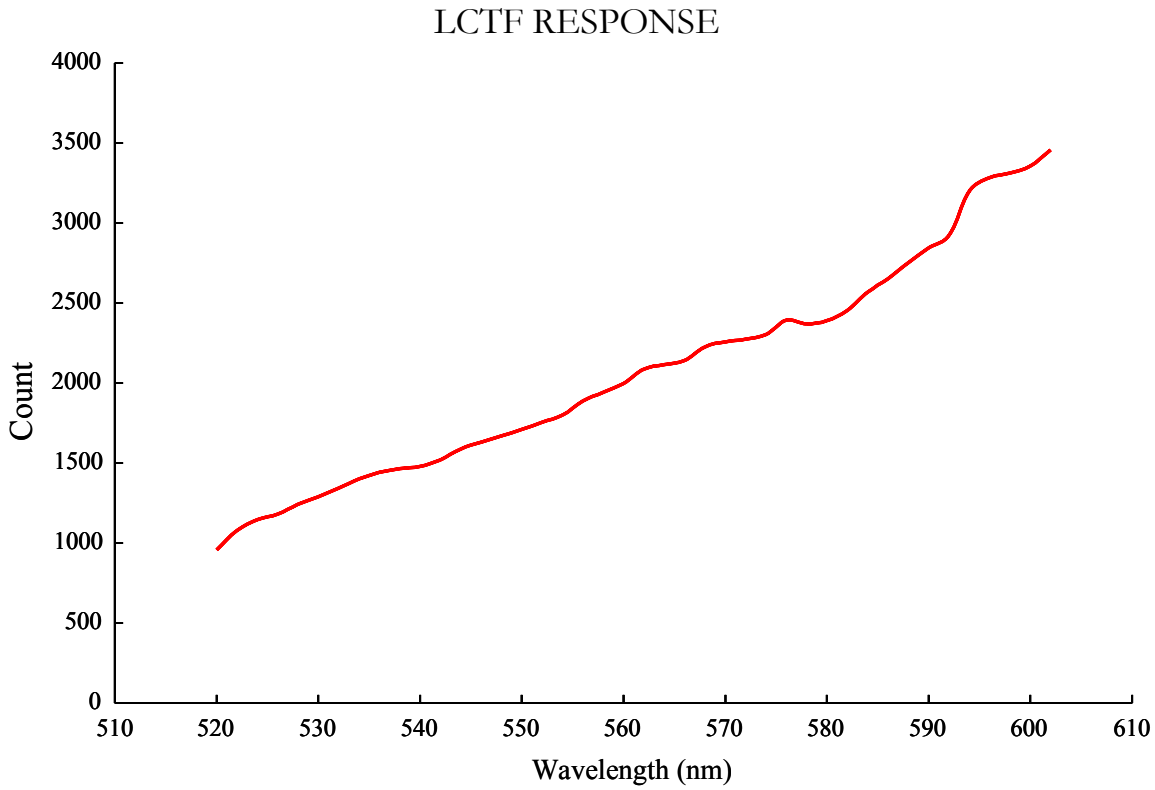

Figure 16: Spectral Output for the microscopic visible hyperspectral imaging system

In the second step, the apparent absorbance spectra, a convolution of the HbO_2 and Hb, are transformed into percentage of HbO_2 by deconvoluting the measured spectra into two intrinsic components. The measured spectrum is deconvoluted by performing a least-squares fit for each detector pixel, to determine the best combination of the HbO_2 and Hb refrence spectra. Using the pure component reference spectra of fully oxygenated hemoglobin (100 % HbO_2) and completely desaturated hemoglobin (100 % Hb), one can

determine the % HbO_2 at each sampling area. The apparent absorbance is given by equation 1 [14].

$$A_{xy}(\lambda) = \log_{10}(R_{xy}(\lambda)_{s\tan dard} / R_{xy}(\lambda)_{sample})$$

Equation 1: Calculation of Apparent Absorbance [14]

Prior to deconvoluting the data cube for relative contribution of HbO_2, the data is filtered using a Savitzky-Golay polynomial filter and then normalized. The Savitzky-Golay filter is a moving window low pass filter that is very helpful in spectroscopic applications. It aids in visualization of the relative height and width of the spectral lines in otherwise noisy spectroscopic data. Instead of operating in Fourier domain, the Sav-Gol filter operates in time domain and smoothen the data [35]. Equation 2 describe the Savitzky-Golay filter,

$$g_i = \sum_{n=-n_l}^{n_r} c_n f_i + n$$

Equation 2: Savitzky - Golay Equation [35]

where, $Cn = \{ (A^T \cdot A)^{-1} \cdot (A^T \cdot f_n) \}$,

$A_{ij} = i^j$, j = 0, 1, 2…..M. M is the polynomial order,

n_l is the number of data points used on the left of point n and

n_r is the number of data points used on the right of point n.

Savitzky Golay filter is not simply a moving window average filter, but instead if replacing g_i by a constant (whose estimate is the average), it uses a polynomial of higher

order, typically quadratic or quartic i.e. for each point f_i, least square fitting is used for all $n_l + n_r + 1$ points in the moving window and then defining g_i at *i*. At f_{i+1}, a whole new least square fitting is done using the shifted window. In equation 2, c_n is the filter coefficients that accomplished this process of polynomial fitting within the moving window and are derived using the matrices and *i* is the pixel location [35]. The window size we are using for data analysis is 15. The filter removes the tail on the either side of the wavelength range hence the useful spectral range is reduced from 520 – 602 nm to 534 – 588 nm.

Finally, after filtering the data, the measured spectrum is deconvoluted for percent values of oxyhemoglobin and deoxyhemoglobin through mulit-variate least square regression analysis to determine the best linear combination of HbO_2 and Hb reference spectra.

CHAPTER 4

RESULT

4.1 System Characterization

The microscopic hyperspectral imager modified and developed for retinal imaging was characterized for imaging performance. The system was optimized for better visualization of the retina and the different components were characterized. The CCD camera was characterized in terms of its spatial resolution. The LCTF was calibrated for its tuning accuracy, tune wait time, bandwidth and the optical transmission. In addition, the slit lamp ophthalmoscope was characterized for the intensity delived to the target at varying the source to target (i.e. retina) distance.

4.1.1 Slit Lamp Source

The slit lamp source provides a broad band of white light initially for illuminating the target. Though the broad band light is filtered in the visible region of light through the LCTF, it was calibrated for the light intensity it produced at varying distances. The LCTF was tuned to 602 nm, where the LCTF has the highest optical transmission. The source intensity was set to its maximum and the measurement was carried out. The light source illuminates a circular area of the target and can be thought to be inversely proportional to the square of the distance between the illuminating prism and the target.

The intensity at varying source distance was measured using a NIST calibrated light meter (Cal-Light 400, Cooke Corporation, MI) with a silicon photodiode sensor, providing direct measurement within 0.1 – 40 Klux [36]. The intensity was measured at a distance from 0 to 8 cm between the target (i.e. light meter) and the illuminating prism. The figure 17 shows the intensity plot for varying source distance.

In figure 17, x – axis represents the distance between the target in this case luxmeter from the illuminating prism and y – axis represents the intensity. The source was moved backward every 1 cm, keeping the luxmeter stationary. The equation between y and x is as shown in figure 17. For imaging the retina, the subject's eye is placed at a distance of about 10 – 12 cm from the source.

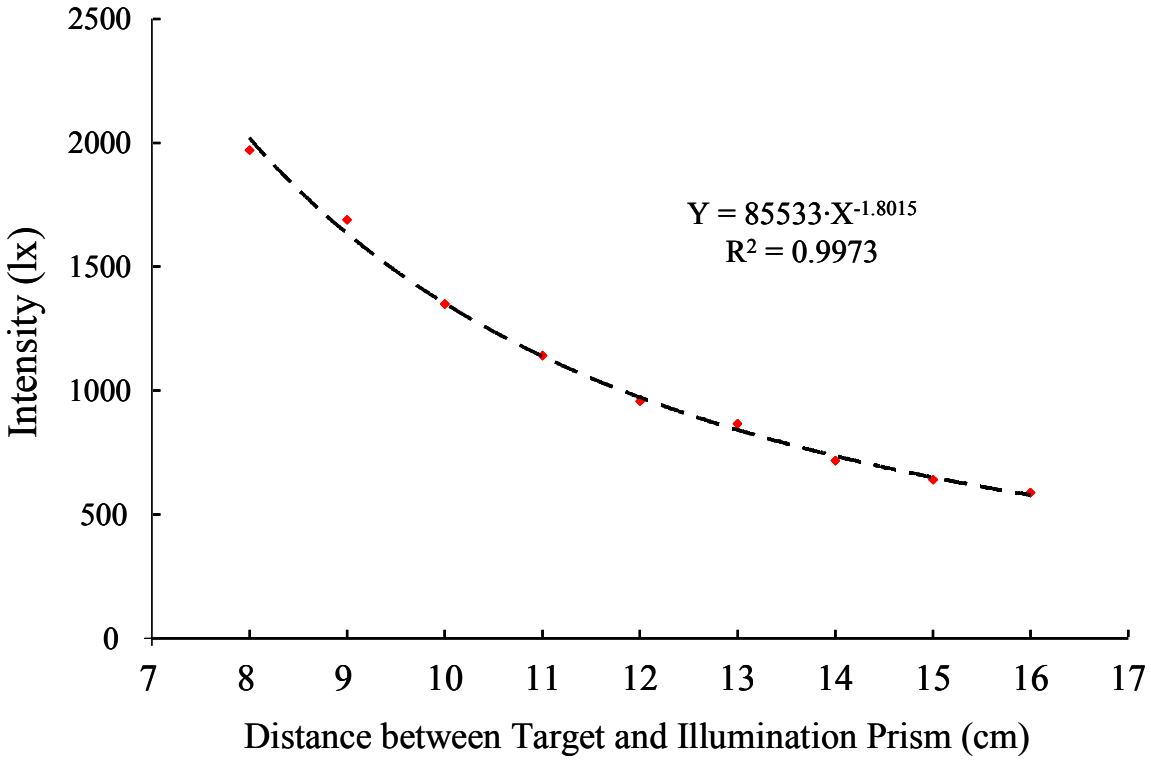

Figure 17: Slit Lamp Source Intensity Versus Distance

The microscopic hyperspectral imager for imaging the human sclera [9] used a broad band white light to illuminate the target. One of the drawbacks of this imaging system was the amount of light that can be shone at the target. The present configuration illuminates the target through the LCTF and we know that the LCTF suffers from low optical transmission. Though LCTF suffers from low transmission, the amount of light shone at the target is far less than that shone without the LCTF in the beam path to the target, Figure 18 and 19. Figure 18 shows the intensity of light measured in lux at the target without the LCTF in the beam path for varying source intensity. From figure 19, it can be appreciated that the light going into the target (retina) is significantly reduced when the LCTF is placed in the beam path. Though the amount of light shown is relatively less, the signal at the detector is not affected by this configuration.

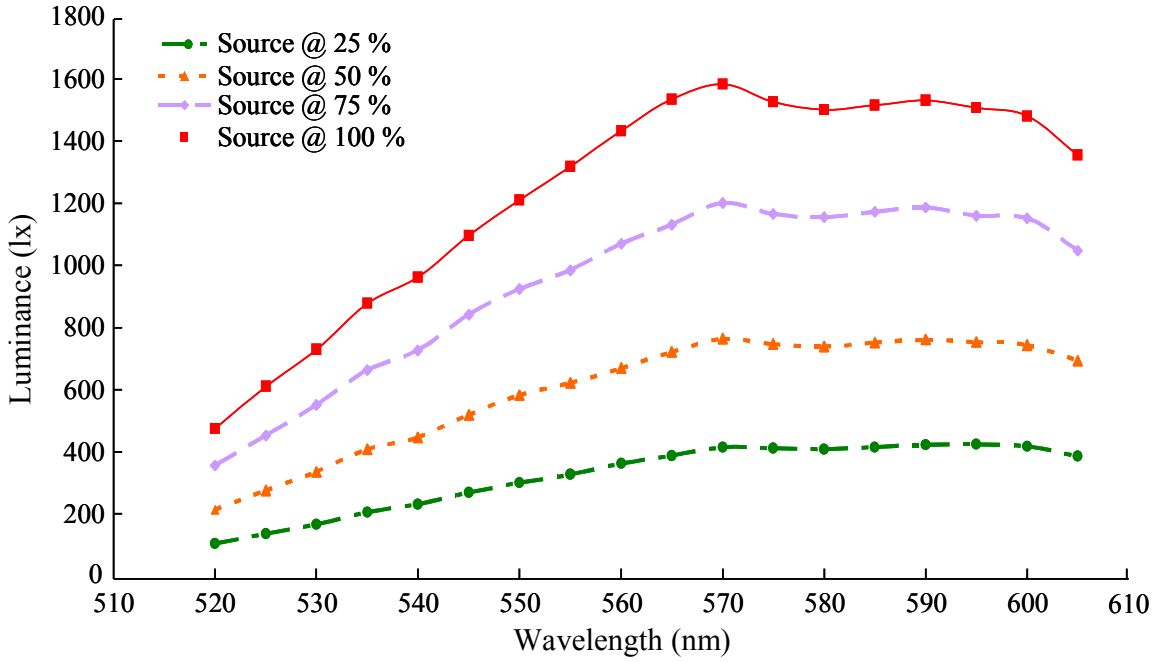

Figure 18: Intensity Measurement at Target with LCTF in the beam path.

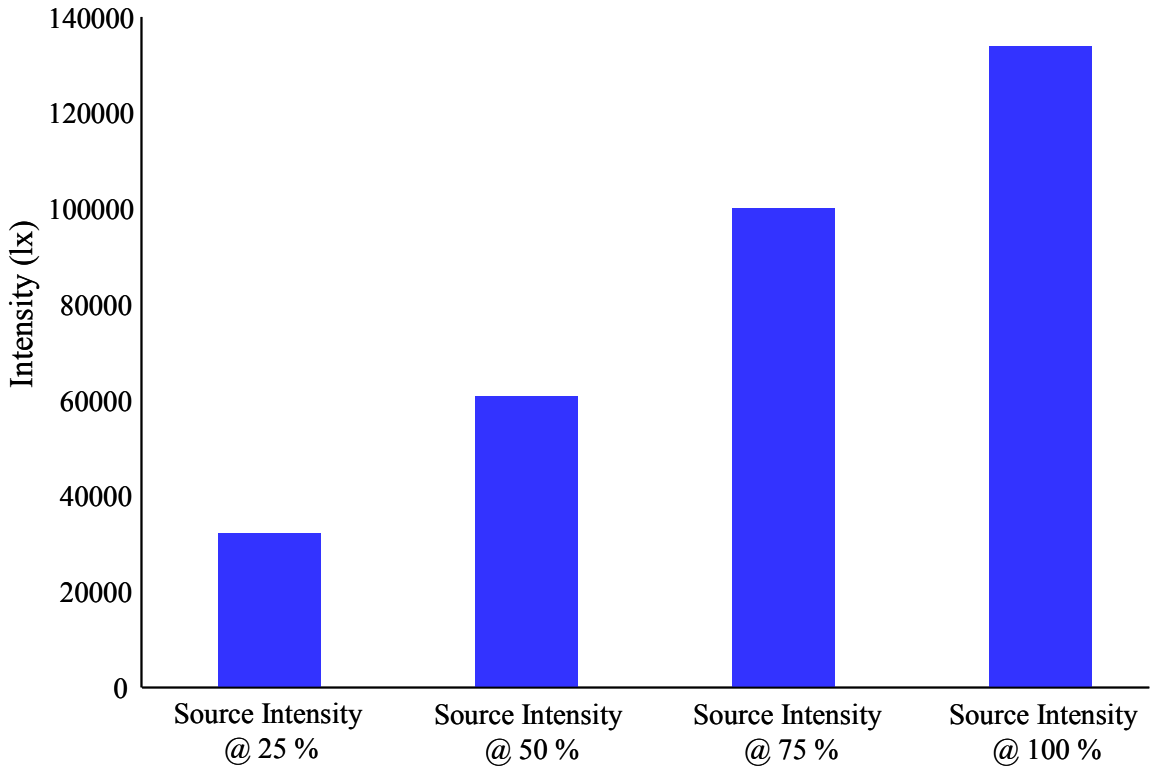

Figure 19: Intensity Measurement at Target without LCTF in the beam path.

4.1.2 LCTF Calibration

The spectral capabilities of the high resolution LCTF were determined using a calibrated Perkin Elmer Spectrometer (Perkin Elmer, USA) from Dr. Liu's Laboratory of Biomedical Optics.

The spectrometer was scanned in increments of 0.1 nm with the high resolution LCTF that was tuned to a specific wavelength placed in the collimated optical path of the spectrometer. The whole range of the LCTF, 480 nm – 720 nm was scanned with an increment of 10 nm and the absorbance spectra were measured. The reciprocal of the absorbance spectra yielded the transmittance spectra at that wavelength. Further, the data

was analyzed using Matlab to measure the centered wavelength the LCTF actually tuned to. Table 5 shows the comparison of the tuned wavelength versus the measured wavelength. As seen the high resolution LCTF tunes within the error of the tuned wavelength.

The figure 20 shows the plot comparing the tuning accuracy. The desired wavelengths to which the LCTF was tuned were sent electronically to the control box and are plotted on the x – axis and the actual centered wavelength that was measured is plotted on y – axis. Linear regression was used to fit the data to get the equation of the line.

Table 5: Comparison between Tuned Wavelength Vs Measured Wavelength

Tuned Wavelength (nm)	**Measured Wavelength (nm)**	**Tuned Wavelength (nm)**	**Measured Wavelength (nm)**
490	489.9	610	609.9
500	499.7	620	619.9
510	509.8	630	629.9
520	519.9	640	639.9
530	529.8	650	649.9
540	539.8	660	659.9
550	549.9	670	670
560	559.8	680	679.9
570	569.8	690	690
580	579.9	700	700
590	589.9	710	710
600	599.9	720	720

Though there exist a small error of the tuned wavelength, the error is rectified by setting up a look-up table in the V++ software from the relationship that we derive which makes sure that the LCTF gets tuned to the wavelength which the operator desires. The high resolution LCTF was not characterized for the spectral band pass that is determined by the Full Width at Half Maximum, FWHM, an expression of the difference between the two extreme values of the wavelength at which the percent transmission is equal to half its maximum value. The high resolution has a spectral band of 0.19 nm at 500 nm and 0.75 nm at 700 nm and is highly dependent on the wavelength [11].

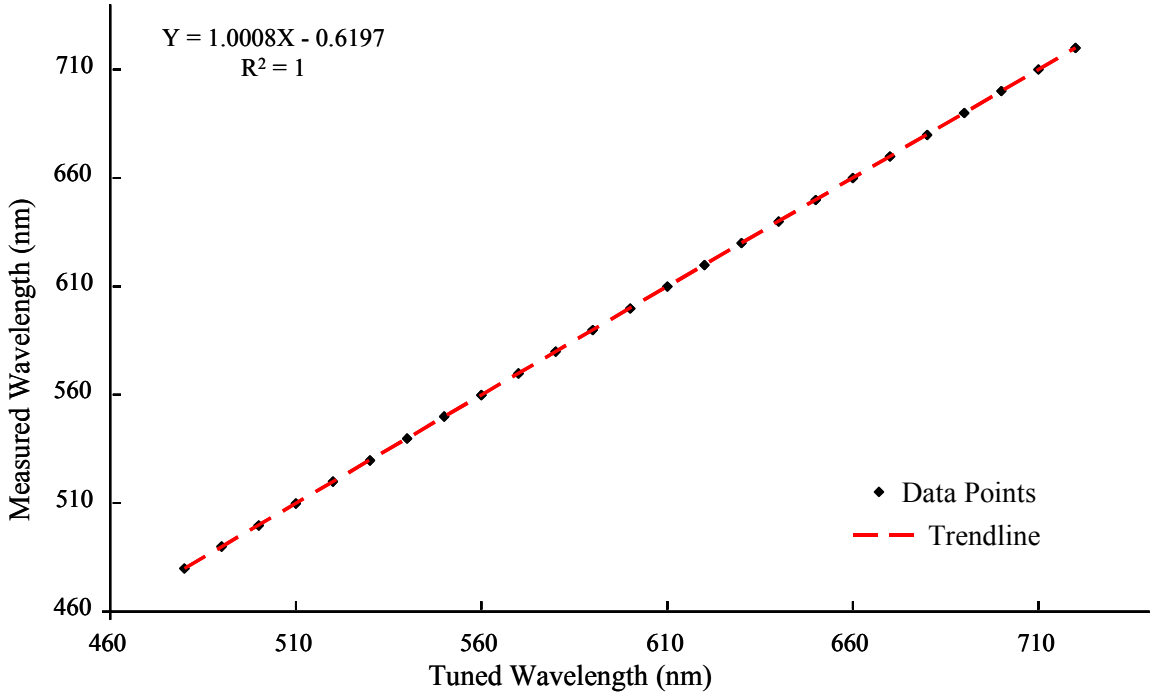

Figure 20: High Resolution LCTF Calibration Curve

Apart from characterizing the high resolution LCTF for tuned wavelength, the visible low resolution LCTF was also characterized for tuned wavelength, spectral band pass, tune delay and the optical transmission. The low resolution LCTF was characterized

for tuning accuracy using the Perkin Elmer spectrometer. The calibration curve is as shown in figure 21. Linear regression was then used to get the relationship between the measured wavelength and the tuned wavelength. From the equation, a look up table was generated in V++ software to offset the error and to tune the low resolution LCTF to the wavelength of interest.

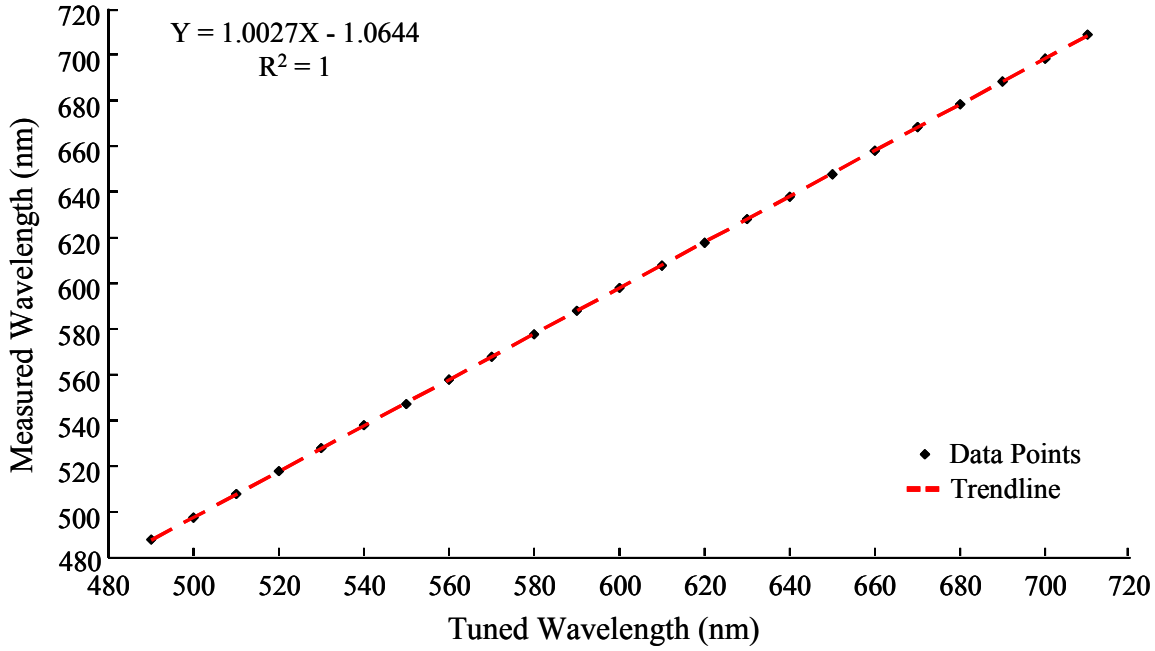

Figure 21: Low Resolution LCTF Calibration Curve (Serial No. 51159)

The bandwidth of the low resoltuon LCTF was determined by using high resolution LCTF as a spectrometer. The experimental setup when using high resolution LCTF as the spectrometer is as shown in figure 22. As shown in figure 22, the light from the source passes through the low resolution LCTF that is tuned to a specific wavelength. The high resolution LCTF scans over the spectral range of the tuned wavelength with an increment of 0.2 nm. The incoming light then passes through the 60 mm Nikon camera lens which focuses the light onto the FPA, generating the hyperspectral cube for each

tuned wavelength of the low resolution LCTF. The whole procedure was repeated across the wavelength range of 500 – 700 nm for low resolution LCTF with an increment of 10 nm.The hyperspectral cubes generated were then analyzed in Matlab to find the center wavelength.

From figure 23, the spectral band pass of the visible LCTF is a function of wavelength and varies from 6.46 nm at 500 nm to 16.03 nm at 710 nm. Though the LCTF wavelength range is from 480 nm – 720 nm, the range 500 – 710 nm is practically used in research and clinical setting. The bandpass is sufficient to spectroscopically resolve peaks of HbO_2 and Hb that have spectral characteristics that are several times broader than the broadest band pass.

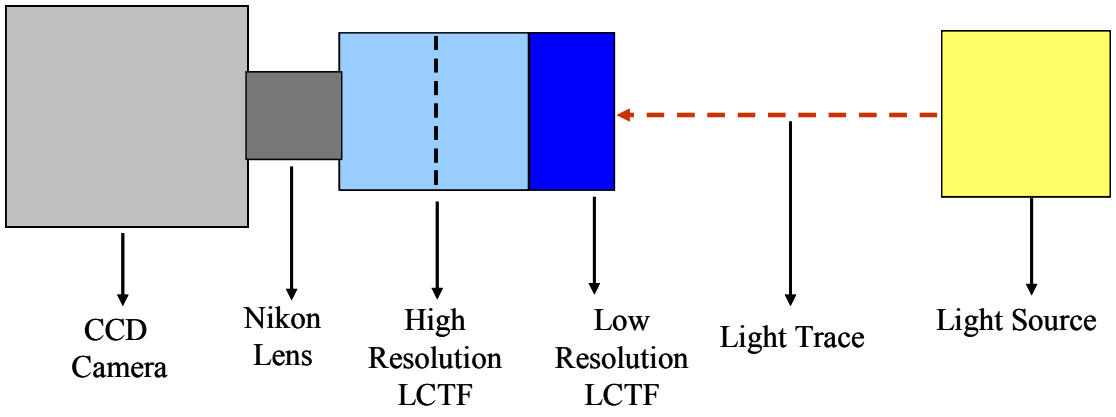

Figure 22: Experimental Setup for Calibrating Low Resolution LCTF

LCTF was optimized for its tune wait time. Tune wait time is defined as the time required by the liquid crystals to settle at a particular wavelength when switched from the previous wavelenght. It typically ranges from 0 ms to 150 ms [23]. Since the hyperspectral image cube is acquired sequentially, the response time is an important experimental parameter. Tune wait time can affect the overall acquisition time, which is

very critical in retinal imaging. A provision has been made in V++ software to set the desired LCTF tune wait time thereby controlling the overall acquisition time.

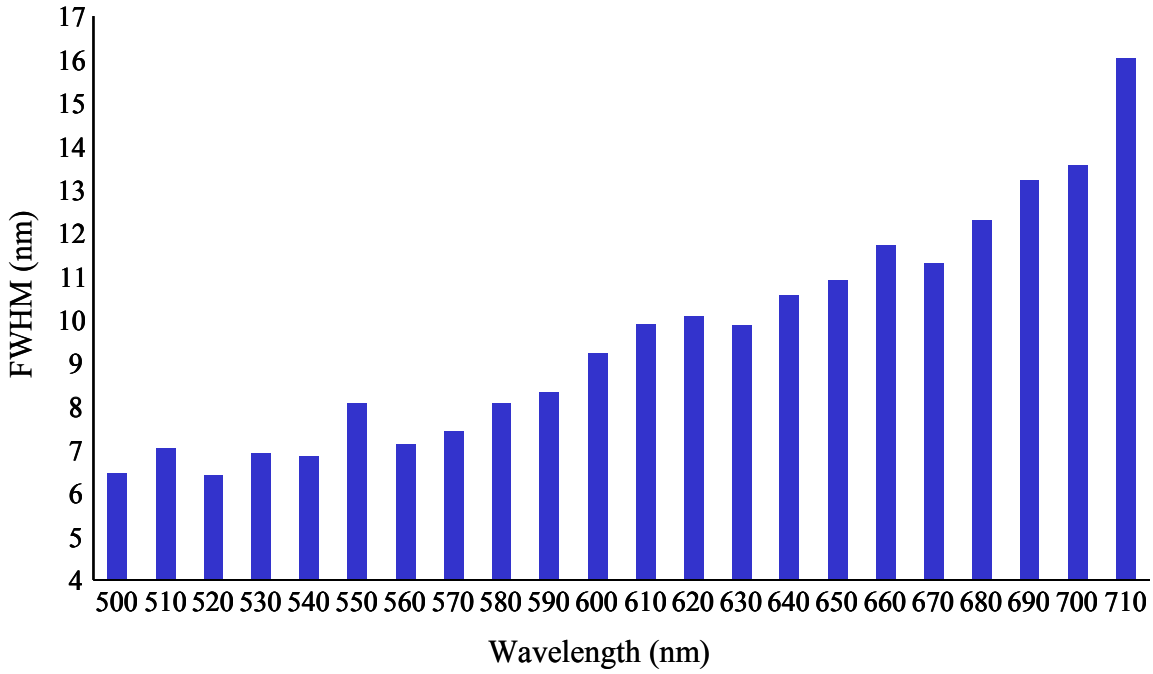

Figure 23: Bandpass plot for Low Res LCTF

An experiment was performed to determine the critical tune time, which will be sufficient for liquid crystals to settle down to the tuned wavelength as well as not have significant effect on the acquisition time. The experimental setup for tune time experiment is as shown in figure 24. As shown, hyperspectral data cubes from the 99 % reflective target were acquired under the constant broad band light excitation. The reflected light from Spectralon^{TM} is focused onto the FPA through the Nikon lens and the LCTF. The hyperspectral cubes are generated for four different tune time: 0 ms, 50 ms, 100 ms and 150 ms. The spectral analysis for these tune time is shown in figure 25. Visually and statistically, there is no difference between the different tune times; thereby

suggesting that setting the tune time to 0 ms will not induce noise in the hyperspectral data.

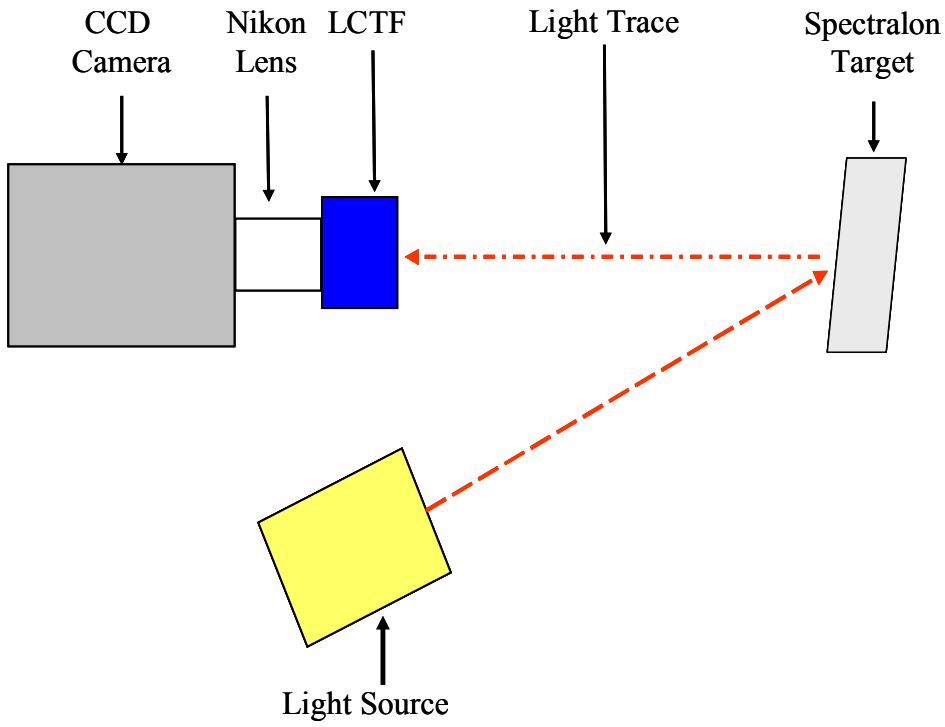

Figure 24: Experimental Setup for Determining Optimum Tune Wait Time

The visible LCTF has low optical throughput and it is important to have a estimate of the same. The experimental setup for measuring the optical throughput at varying wavelength is as shown in figure 26. A baseline hyperspectral data cube was acquired without the low resolution visible LCTF in the light path, that was reflected from the 99 % reflective target. Next, the low resolution LCTF was kept in front of the high resolution LCTF and tuned to a specific wavelength. The data cubes were then acquired through the high resolution LCTF scanning across 480 – 720 nm with an increment of 2 nm. The low resolution LCTF was tuned from 500 – 720 nm with an increment of 10 nm, while acquiring the cube. The resultant plot of optical transmission

is shown in figure 27. The optical throughput at each wavelength was determined by rationing the measured intensity with and without low resolution LCTF in the light path.

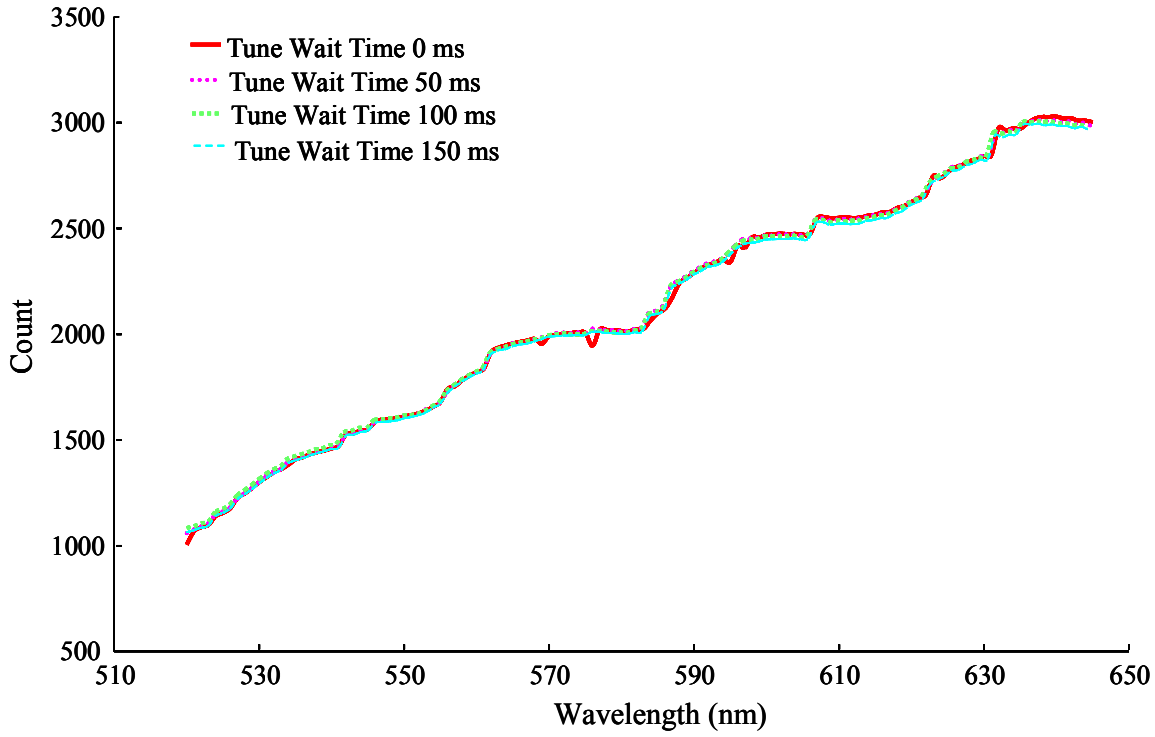

Figure 25: Plot of Different Tune Wait Time

It can be concluded from figure 27 that, the optical throughput is wavelength depended and increases as one moves towards the higher end. Moreover the optical transmission as measured using has a similar profile to the tranmssion as mentioned in the manufacturer's manual.

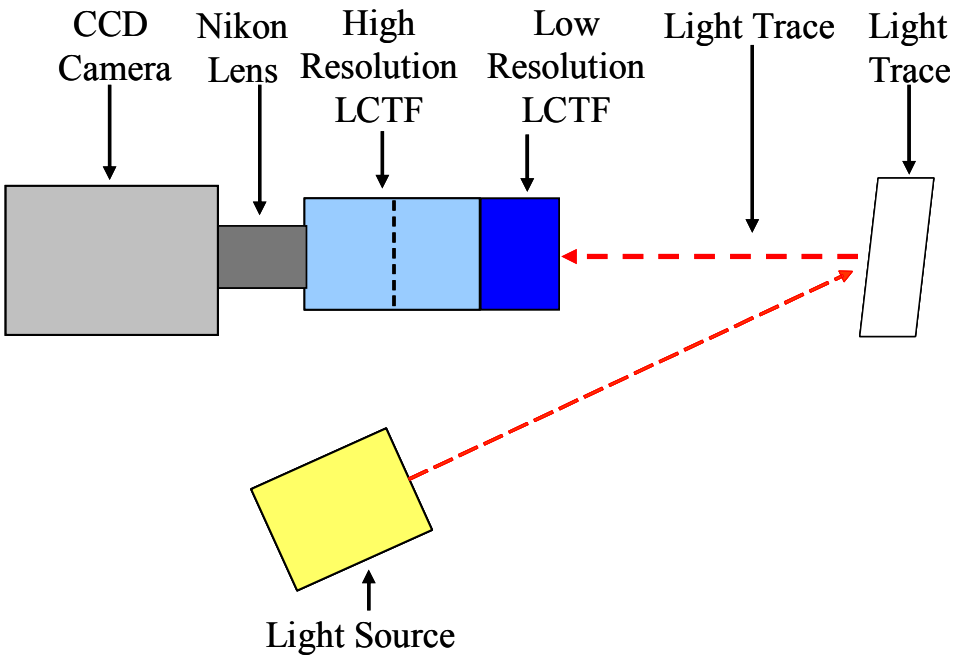

Figure 26: Experimental Setup For Determining the Transmission through Low Resolution LCTF

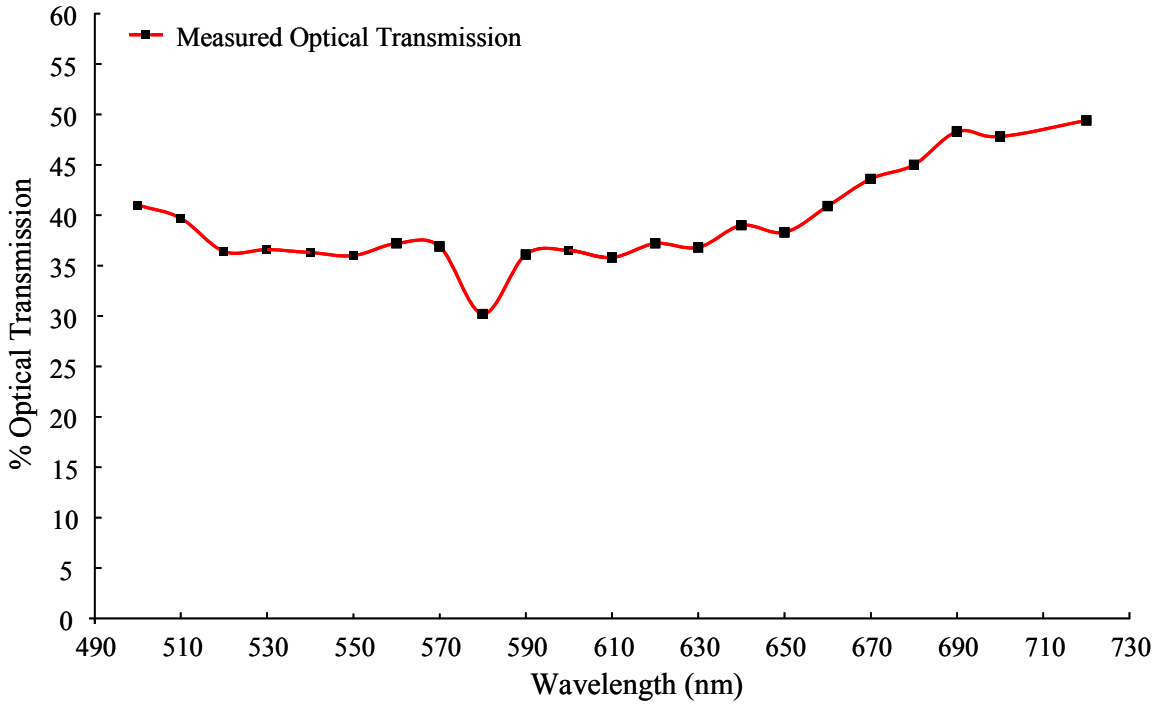

Figure 27: Percent Transmission for the Low Resolution LCTF

4.1.3 CCD Characterization

The spatial resolution of the microscopic hyperspectral imager was determined using a USAF 1951 resolution target. Spatial resolution is defined as the ability of the system to differentiate between two closely spaced points on the image. The spatial resolution of the hyperspectral imager was determined by computing the percent contrast of the various line pairs per millimeter of the resolution target. For the present configuration of the hyperspectral imager, the spatial resolution is dependent on the depth of field, f-stop on the ophthalmoscope, degree of pixel binning and the camera itself. Changing any of these factors alters the spatial resolution of the system. The spatial resolution was measured for different binning parameters and magnification of the ophthalmoscope.

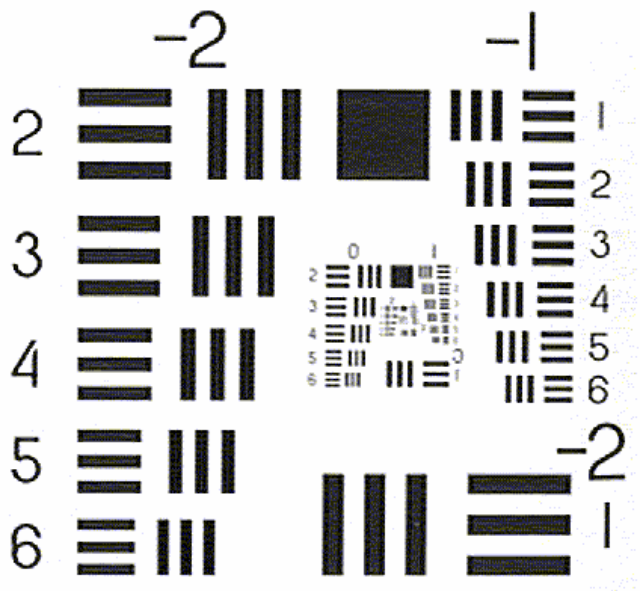

Figure 28: USAF 1951 Positive Resolution Target

A 1951 Quartz USAF (Edmund Optics, Barrington, NJ) positive resolution target, figure 28 was used for measuring the percent contrast. The figure 29 shows a part of

resolution target along with reflected intensity taken along a row of pixel. This intensity profiles provides the percent contrast and hence the spatial resolution of the hyperspectral imager. The Percent Contrast (C) was determined from the expression equation 3, and plotted as a function of spatial resolution in millimeter.

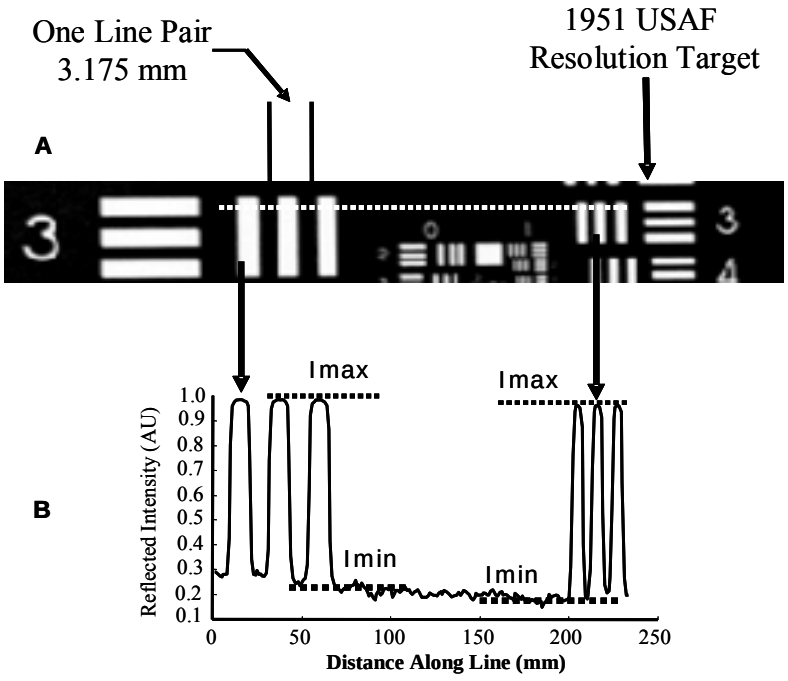

Figure 29: A)1951 USAF resolution target. B) Reflected Intensity plotted for the dotted line in A.

$$C = \left(\frac{I_{\max} - I_{\min}}{I_{\max} + I_{\min}} \right) \times 100$$

Equation 3: Percent Contrast Determination

where, $\boldsymbol{I_{max}}$ = Maximum intensity reflected by a bright line of the resolution target (white bar) and $\boldsymbol{I_{min}}$ = Minimum intensity reflected from the non-reflecting area between the lines (dark bar) of the resolution target as shown in figure 29. The specification for the USAF resolution target is as shown in table 6.

Table 6: Specification Table of 1951 USAF Resolution Target

Number of Line Pairs / mm in USAF Resolving Power Test Target 1951										
Group Number										
Element	-2	-1	0	1	2	3	4	5	6	7
1	0.25	0.50	1.00	2.00	4.00	8.00	16.00	32.00	64.00	128.00
2	0.28	0.56	1.12	2.24	4.49	8.98	17.95	36.00	71.80	144.00
3	0.32	0.63	1.26	2.52	5.04	10.10	201.60	40.30	80.60	161.00
4	0.35	0.71	1.41	2.83	5.66	11.30	22.62	45.30	90.50	181.00
5	0.40	0.79	1.59	3.17	6.35	12.70	25.39	50.80	102.00	203.00
6	0.45	0.89	1.78	3.56	7.13	14.30	28.50	57.00	114.00	228.00

Generally, the spatial frequency, or number of line pairs, where a line pair is defined as one white and one dark bar, increases (the number of pairs / unit length) as the percent contrast decreases [14]. To obtain the percent contrast, the resolution target was placed in the imaging path and an image was acquired. The whole procedure was repeated for 4 different bin settings and different order of magnification. The different images acquired are analyzed for percent contrast and plotted as a function of spatial resolution. (mm). Figures 30 through 32 shows the plot of Percent Contrast versus Spatial resolution where the former is dependent variable y, and the latter is independent variable x. The spatial resolution is determined when the regression model cross the 26 % contrast threshold set by the Rayleigh criterion (dashed line).

Figure 30 shows the spatial resolution for a magnification of 10X. A 1 X 1 binning represented by diamonds, utilizes the entire CCD chip producing am image of 1392 X 1040 pixels. Similarly, the squares, triangles and crosses represent a binning of 2 X 2 (694 X 518 pixels), 3 X 3 (463 X 345 pixels) and 4 X 4 (348 X 260 pixels) respectively. The regression equation for bin 1 X 1 is given as $y = -394.64x^2 + 365.33x + 7.69$. For the same magnification (10X), the regression equation for bin 2 X 2 is $y = -389.25x^2 + 358.89x + 6.0743$. Similarly for bin 3 X 3 the regression fit is given as $y = -443.68x^2 + 407.23 - 8.9806$ and $y = -604.77x^2 + 489.63x - 20.273$ for bin 4 X 4. Similarly, figure 31 and 32 shows the spatial resolution of the system when the magnification is 16X and 25X respectively.

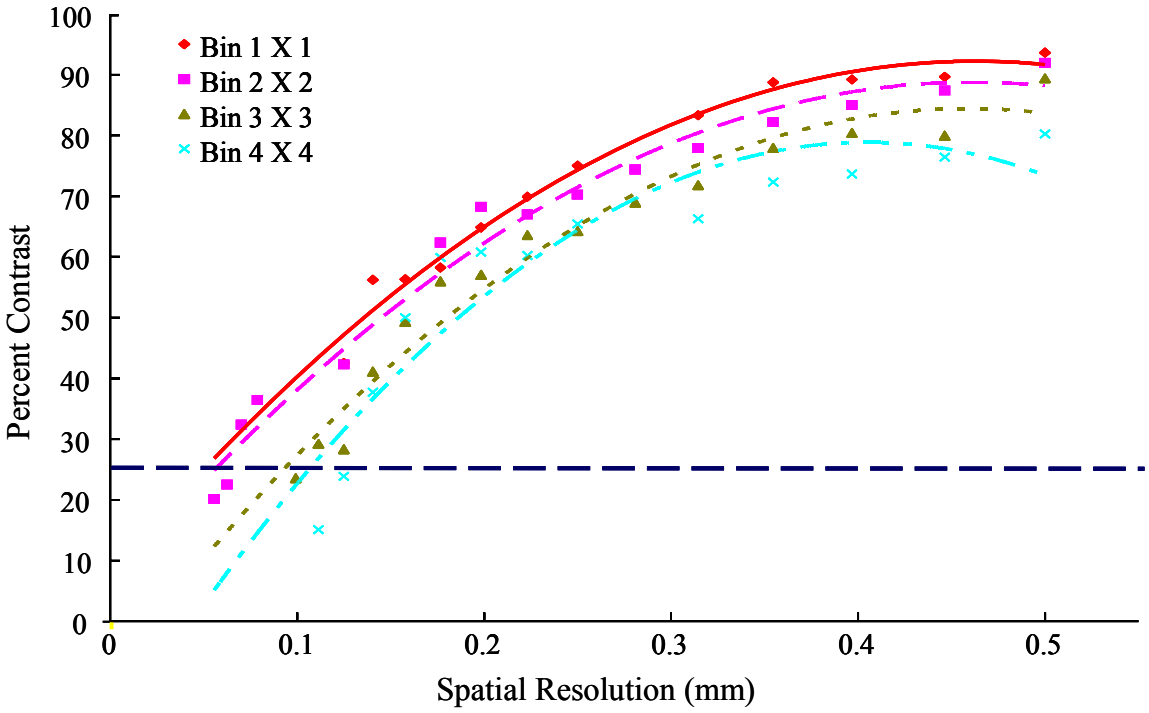

Figure 30: CCD Spatial Resolution for Magnification of 10 X and Different Binning

As per the Rayleigh criterion, the spatial resolution of the imager when the magnification is 10X and binning is 1 X 1 is 0.053 mm. Similarly, spatial resolution is 0.06 mm, 0.096 mm and 0.11 mm at a binning of 2 X 2, 3 X 3 and 4 X 4. These numbers supports the fact that increasing the binning causes the spatial resolution to go down. The spatial resolution is sufficient for clinical examination of the retina.

Similarly for magnification of16X, the spatial resolution was 0.022 mm for bin of 1 X 1, 0.037 mm for bin of 2 X 2, 0.046 mm for bin of 3 X 3 and 0.063 mm for bin of 4 X 4. It can seen that increasing the magnification increases the overall spatial resolution, but the trade – off being the field of view.

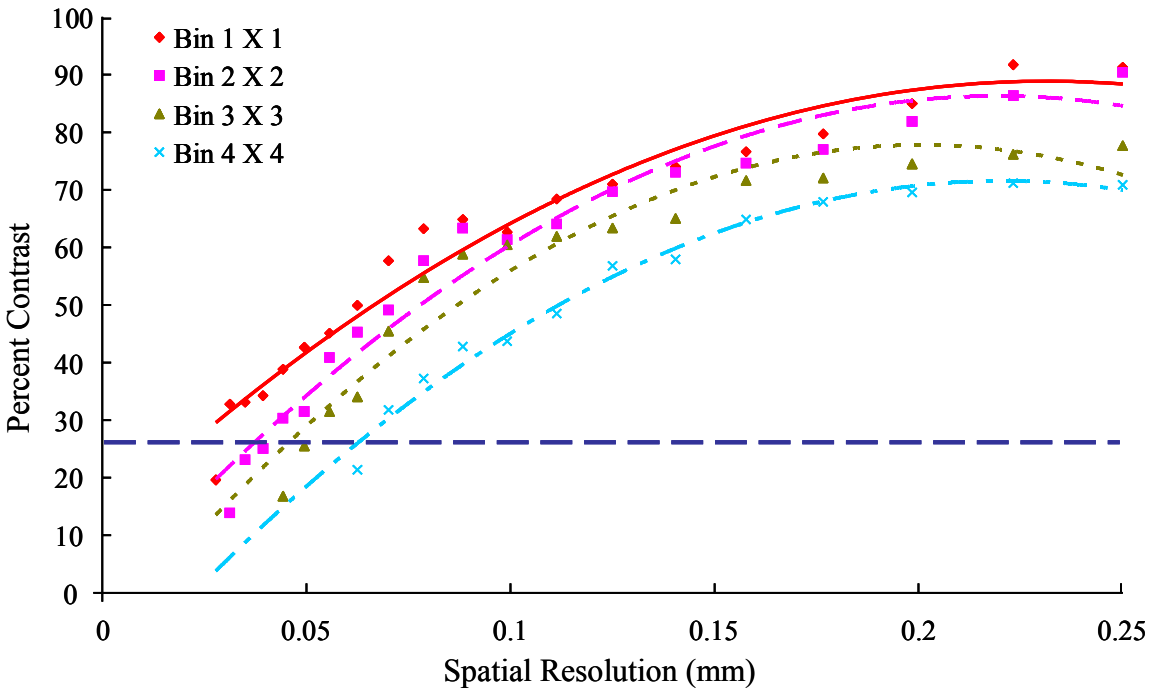

Figure 31: Spatial Resolution Plot for Magnification of 16X

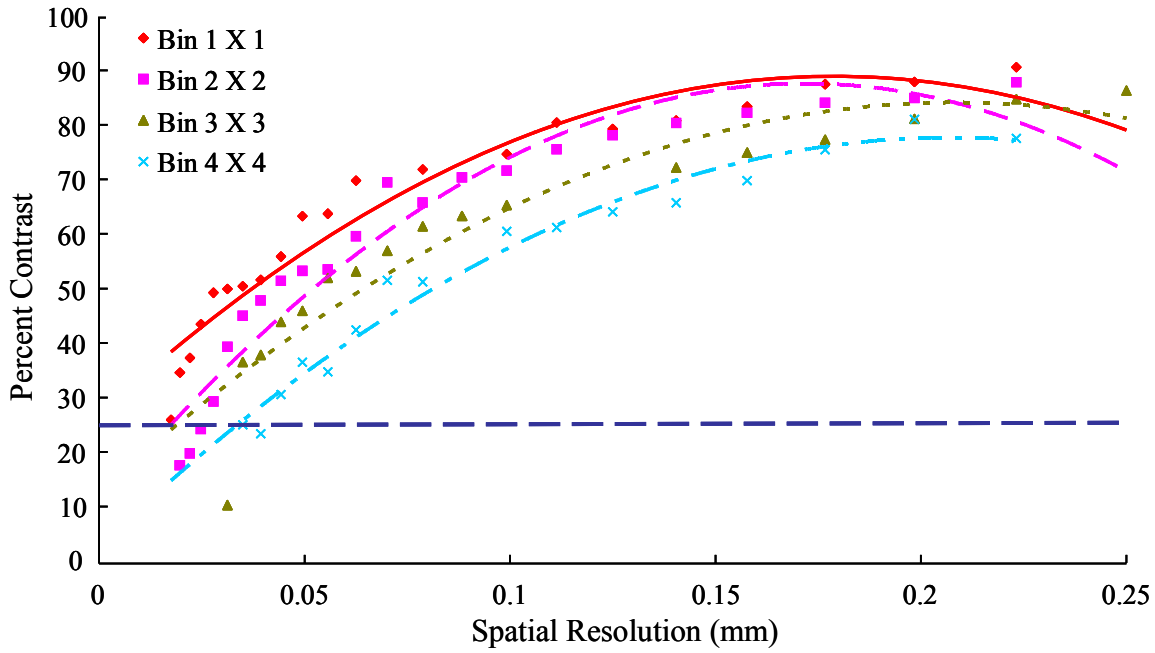

Figure 32: Spatial Resolution Plot for Magnification of 25X

4.1.4 Spectralon Comparison

Spectralon™ is a 99 % diffuse reflectance target that we use as a reference in all our measurement. It gives highest diffuse reflectance in the UV-VIS-NIR region of the spectrum and exhibits highly lambertain behavior [38].

Spectralon exhibits ageing effect resulting in degradation of % reflectance over a period of time [39]. This ageing effect can be manifested as reduction in photon count by FPA. Two spectralon that were purchased over a period of 4 years; first one bought in 2003 and the second one in 2007 are used to check if there is degradation in old reflectance target as compared to the new target.

Experimental setup as shown in figure 24 was used to measure the reflectance profile from both the spectralon. The 99 % reflective target was illuminated by the QTH

light source and the reflected light was filtered through the LCTF which focused the light onto the CCD. The CCD had a gain of 2, exposure time of 8 ms and was binned 4 x 4. The LCTF scanned from 520 to 645 nm by 1 nm increment.. To test the significance, 10 samples were selected from both the data cube. Two separate analyses was done on the data 1) to test if there is a significanct difference between the two set of measurements and 2) if we can correlate the old Spectralon™ and the new Spectralon™ and somehow compensate for the degradation effect by incorporating a regression equation between them. The old and the new reflectance target can be correleated as,

$$y_{old} = 0.998 \bullet y_{new} - 39.386 + 0.07 \bullet \lambda$$

Equation 4: Correlation between the old and the new reflectance target

Statistically, the slope and the intercept (-39.386) showed a significant difference between the old and the new target, but not the wavelength. Thus, regardless of wavelength, there exists a significant difference between the mean intensity values of new and old reflectance target. The p-value for mean intensity of y_{new} – mean intensity of y_{old} is < 0.001 with a difference of 9.8375 and a standard error of 1.01.

4.1.5 Effect of Savitzky Golay filtering for variable sampling rate

As mentioned in chapter 3, Savitzky – Golay filter is utilized to smoothen the hyperspectral data and reduce the noise. The Savitzky – Golay filter is an extension of moving window-averaging filter that preserves the width of the spectrum but reducing the height [35]. An experiment was performed to determine whether Savitzky – Golay filter affects the width of the spectrum (FWHM) and the center wavelength for varying

sampling rate. Experimental setup as shown in figure 5 was used to collect data for three different wavelength (550 nm, 610 nm and 640 nm), within the operating range of visible spectrum and sampling rate varying from 0.2 nm to 4 nm. The collected data was then analyzed statistically to test the significance, whether Savitzky – Golay filter affects FWHM and the center wavelength.

Mixed Linear Model analysis [40] was done to determine if there is a significant difference between filtered FWHM and non-filtered FWHM. Similar test was done to determine if there is a significant different between the filtered center wavelength and unfiltered center wavelength. A summary of t-stat, P-values, standard error and difference in means is shown in table 8 below.

Table 7: Comparison of t-value for 3 sets of wavelength and different sampling rate for FWHM

Wavelength (nm)	Sampling Rate (nm)	Difference in mean	Standard Error	t value	Significant Difference
550	0.2	-0.055	0.046	-1.200	No
	0.3	0.217	0.207	1.050	No
	0.4	0.237	0.043	5.570	No
	0.5	0.267	0.056	4.720	No
	0.6	0.412	0.055	7.500	Yes
	0.7	0.728	0.019	39.000	Yes
	0.8	1.080	0.012	88.420	Yes
	0.9	1.310	0.046	28.270	Yes
	1	1.792	0.072	24.980	Yes
610	0.2	-0.154	0.024	-6.480	Yes
	0.3	-0.002	0.013	-0.180	No
	0.4	0.048	0.006	8.150	Yes
	0.5	0.170	0.024	6.940	No
	0.6	0.207	0.012	17.830	Yes
	0.7	0.274	0.030	9.160	Yes
	0.8	0.402	0.072	5.550	No
	0.9	0.630	0.021	30.080	Yes
	1	0.987	0.012	83.170	No

Table 7: Continued

640	0.2	-0.140	0.079	-1.790	No
	0.3	0.656	0.369	1.780	No
	0.4	0.232	0.093	2.490	No
	0.5	0.243	0.109	2.230	No
	0.6	0.194	0.179	1.080	No
	0.7	0.399	0.176	2.270	No
	0.8	0.521	0.163	3.200	No
	0.9	0.732	0.036	20.280	Yes
	1	0.983	0.177	5.560	No

We have used Scheffe's multiple comparison procedure and controlled the family wise Type I error rate to $\alpha = 0.05$. Table 9 shows the results for effect of Savitzky – Golay filter on the center wavelength.

Table 8: Comparison of t-value and significant difference for the effect of Savtizky - Golay filter on the center wavelength for different sampling rate

Wavelength (nm)	**Sampling Rate (nm)**	**Difference in Mean**	**Standard Error**	**t -value**	**Significant Difference**
550	0.2	-0.200	0.000	~ 0	No
	0.3	-0.200	0.163	-1.220	No
	0.4	0.000	.	.	No
	0.5	-0.167	0.136	-1.220	No
	0.6	-0.200	0.163	-1.220	No
	0.7	0.233	0.191	1.220	No
	0.8	-0.067	0.054	-1.220	No
	0.9	0.000	.	.	No
	1	0.000	.	.	No
610	0.2	-0.400	0.000	~ 0	No
	0.3	-0.600	0.245	-2.450	No
	0.4	-0.533	0.109	-4.900	No
	0.5	-0.167	0.136	-1.220	No
	0.6	-0.200	0.163	-1.220	No

Table 8: Continued

610	0.7	-0.233	0.191	-1.220	No
	0.8	-0.267	0.218	-1.220	No
	0.9	-0.600	0.245	-2.450	No
	1.0	-0.667	0.272	-2.450	No
640	0.2	-0.200	0.163	-1.220	No
	0.3	0.233	0.191	1.220	No
	0.4	-0.067	0.054	-1.220	No
	0.5	0.000	.	.	No
	0.6	1.000	0.163	6.120	No
	0.7	1.167	0.191	6.120	No
	0.8	0.800	0.000	~ 0	No
	0.9	0.900	0.000	~ 0	No
	1.0	0.000	0.471	0.000	No

From table 9, there is no significant difference between filtered center wavelength and unfiltered center wavelength. From this, it can be inferred that, the Savitzky – Golay filter does not shift the peak(s) of the spectra from the theoretical values. Figure 33 displays the plot of Mean FWHM versus different sampling rate for all the 3 wavelengths.

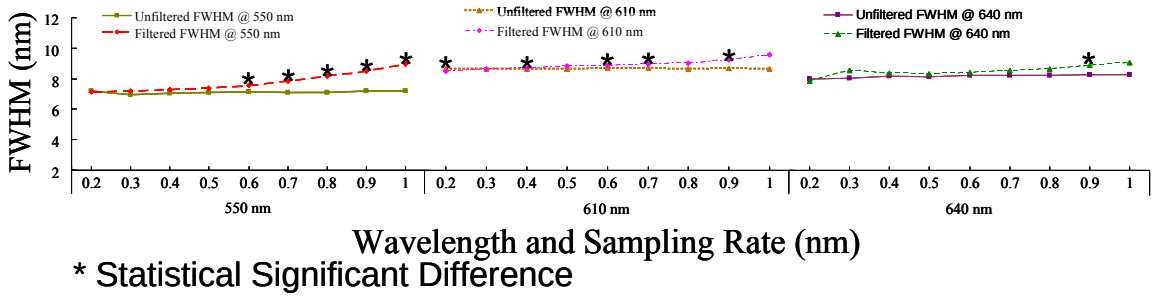

Figure 33: Plot of FWHM Versus Sampling Rate for 3 different Wavelength

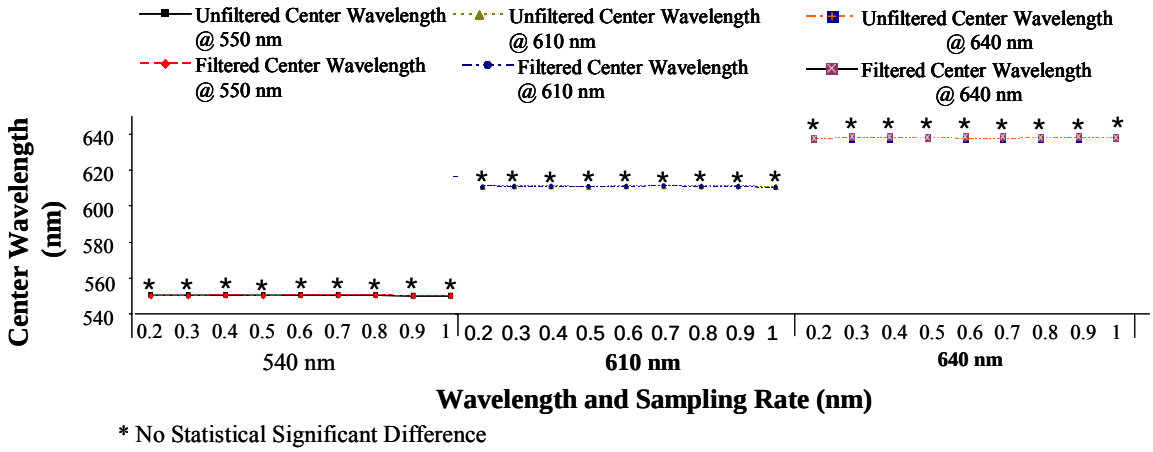

Figure 34: Plot of Center Wavelength versus Sampling Rate
for 3 Different Wavelengths

From figure 34, it can concluded that Savitzky Golay Filter does not shift the center wavelength.

4.2 Retinal Imaging and Analysis

As mentioned earlier, Hyperspectral imaging has the capability of monitoring tissue oxygenation and provides both spectral and spatial characteristics. To demonstrate the capabilities of the microscopic hyperspectral imager, a human retina was image with the present configuration in the visible spectrum, 520 – 602 nm. The image was acquired with a magnification of 10X, bin of 4 X 4 and wavelength range of 520 – 602 nm with a wavelength increment of 2nm. The overall image acquisition time with these parameters was less than 5 seconds, which is critical for imaging eye. Prior to imaging the retina, the subject was administered the pupil dilating drops tropically for opening up the pupil in order to visualize the retina using the diopter lens and the ophthalmoscope. Figure 35A shows a hyperspectral retinal image deconvoluted for oxyhemoglobin contribution values

that are grayscale encoded and spatially depicted. As seen in figure, brighter the pixel greater the oxyhemoglobin contribution as depicted by gray scale bar associated with the image. Moreover a small region depicted in violet box as selected within which the pixel were averaged and the spectrum was plotted. Since the region has a lower intensity value, the associated spectrum resembles deoxyhyemoglobin spectrum, Figure 35B. Figure 35C reveals the oxyhemoglobin spectrum with corresponding pixel intensity being brighter then violet region.

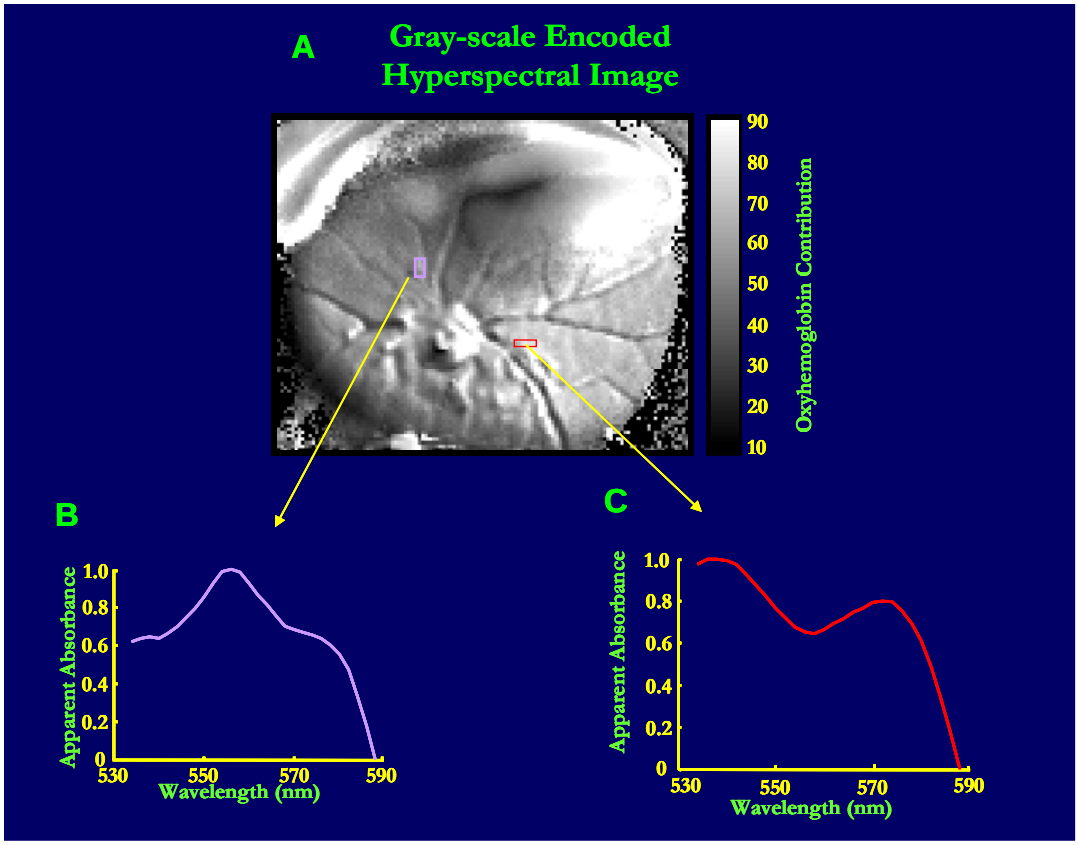

Figure 35: Microscopic Hyperspectral Imaging of the eye. A) Grayscale encoded image showing oxyhemoglobin contribution values as a function of space. B) Spectroscopy from the violet box region resembling oxyhemoglobin curve. C) Spectroscopy over a red box region resembling strong oxyhemoglobin reference curve

Since only a single subject was imaged to show the capabilities of the microscopic hyperspectral imager, the oxyhemoglobin contribution over different areas from single image was calculated and shown in table 8. The selection of region was not randomized but was based on the spectroscopic result yielded over the selected region. The numbers presented in table 7 are all relative to each other and demonstrates that there exists marked differences between oxygenated and deoxygenated areas within the retina and its associated structures.

Table 9: Oxyhemoglobin contributions in retina

	% HbO_2 Contribution over an assumed arterial region (Mean ±SEM)		% HbO_2 Contribution over an assumed venous region (Mean ±SEM)
Area 1	57.947 ± 0.791	Area 2	32.741 ± 1.227
Area 3	56.287 ± 1.361	Area 4	33.078 ± 0.987
Area 5	63.905 ± 1.061	Area 6	37.897 ± 0.883

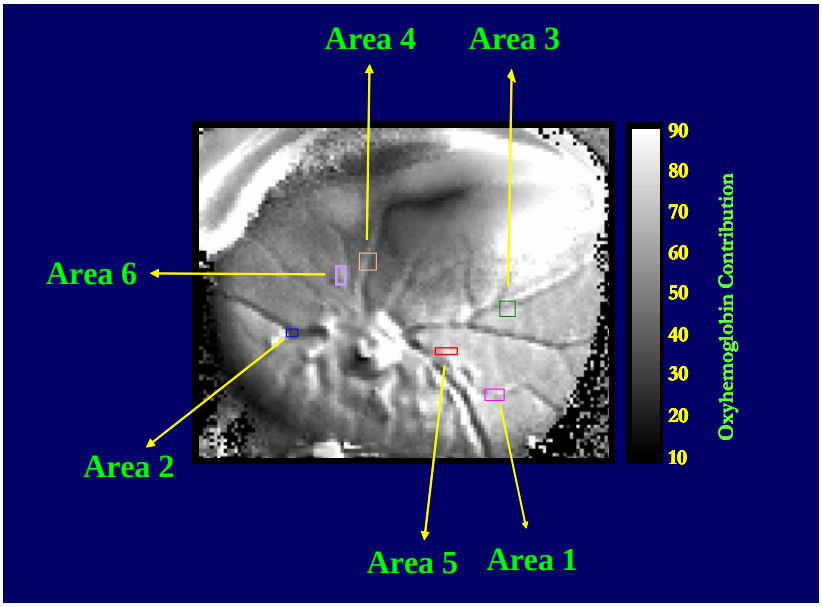

Figure 36: Gray Scale encoded image indicating the areas for computing the % HbO_2 and % Hb

CHAPTER 5

DISCUSSION

Hyperspectral imaging, has been widely used in military and remote sensing application, however its use in medical diagnosis is relatively new. Hyperspectral imaging integrates spectroscopy with spatial imaging thereby rendering spectral information at pixel level. The microscopic hyperspectral imager developed at UTA could prove to be a versatile instrument for ophthalmologist, helping in diagnosis of serious eye diseases.

To begin with the components of microscopic hyperspectral imager were characterized and optimized for efficient functioning of the system and providing accurate results. The slit lamp ophthalmoscope providing high magnification with a binocular vision was characterized for the lamp source intensity, to find out that the intensity level is well within the acceptable limit in patient safety.

The LCTF that filters the broad band light into different wavelengths of light in the visible spectrum was calibrated to make sure that it tunes well to the selected wavelength. Next spectral resolution was characterized at number of wavelengths in the commonly used wavelength range. The LCTF was also characterized for tune wait time delay and an for optimum acquisition time, it was set to be 0 ms. Last but not the least LCTF was characterized to compute its transmission efficiency and it was found out to be 30 % – 55 % in the range of 500 – 720 nm. We have significantly reduced the level of

intensity shone at the target by using the LCTF as a light source as compared to using it in front of the FPA.

The focal plane array, CoolSNAP$_{ES}$ a 1392 x 1040 array provides better spatial resolution and quantum efficiency, which is extremely important when imaging the microvasculature and especially the retina. The CoolSNAP$_{ES}$ uses a 20 MHz digitizer making the data acquisition faster thereby minimizing the movement of the eye and smaller acquisition time. The CoolSNAP$_{ES}$ employs a binning of 4 and provides spatial resolution of 0.11 mm. The macroscopic system developed at UTA has the capability to scans across a range of 520 – 645 nm by 1 nm increment, however to speed up the acquisition without compromising the spectra detail, the microscopic hyperspectral imager scans across a range of 520 – 602 nm with an increment of 2 nm.

After characterizing the system components the human retina was imaged to obtain a hyperspectral data cube that upon deconvolution with the reference spectra of oxyhemoglobin and deoxyhemoglobin in the visible range rendered a gray scale encoded image which showed spatially distributed contributions of oxyhemoglobin.

CHAPTER 6

CONCLUSION AND FUTURE GOALS

The microscopic hyperspectral imager is developed and characterized at UTA to determine the relative oxyhemoglobin and deoxyhemoglobin contribution in the retina non-invasively and *in-vivo*. As a proof of principle, a single subject clinical study was done to demonstrate the capability of the present system to visualize and deconvolute the % of HbO_2 in the retina.

The present system, though capable of imaging retina, can be further enhanced for better results. For example, the present configuration utilizes a relatively small filed of view. By integrating the relay optics and a camera lens, the image can be blown up to utilize the whole CCD chip. The major advantage of using relay optics is the utilization of the fully chip and possibly improving the spatial resolution from the present configuration.

Also diopter lens is manually operated to visualize retina which is not desirable in clinical setting, as will induce small movement artifact. The diopter lens can be machined and integrated with the opthalmoscope and be either manually or electronically operated for viewing the retina. Movement artifacts within the subject's eye are hard to control and hence an algorithm filtering the movement artifacts will be extremely useful.

In addition to above two enhancement, a high sensitive camera can be used to visualize the retina. Using a high sensitive camera can provide better spatial resolution, reduce acquisition time and higher sensitivity.

Currently plans are underway to use the present system to image the retina of the mice under variety of physiological conditions. This will help to calibrate the system to provide the % HbO_2 and % HbO values within the acceptable limit. Moreover imaging the mice retina, will help to differentiate the spectral signatures of the other sub structures within the retina.

Last but not the least, DMD chips can be integrated with the present system to use it as a light source with varying wavelengths and thereby replacing the LCTF in hyperspectral imaging system.

APPENDIX

A. UTA IRB FORM

UNIVERSITY OF TEXAS AT ARLINGTON
OFFICE OF RESEARCH COMPLIANCE

IRB FORM #1

INITIAL SUBMISSION OF A RESEARCH PROTOCOL TO THE INSTITUTIONAL REVIEW BOARD FOR THE PROTECTION OF HUMAN SUBJECTS

Faculty, staff, students, or employees who propose to engage in any research, demonstration, development, or other activity involving the use of human subjects must have review and approval of that activity by the Institutional Review Board, prior to initiation of that project. The Board is responsible for safeguarding the rights and welfare of subjects who participate in the activity.

If you require further assistance in completing this form or need additional information, please contact the Office of Research Compliance at extension 3723.

SECTION A: GENERAL INFORMATION

1. **Project Title:** In-vivo Visible Reflectance Hyperspectral Imaging of Retina

2. **Principal Investigator:**

   - **Name**: Nirad Zinzuwadia
   - **Title:** Graduate Student
   - **Department:** Bioengineering, UTA **Mail Box**: 19138
   - **Telephone**: 817-272-0809 **Email**: niradzinzuwadia@hotmail.com

3. **Co-Investigator:**
   - **Name**: Dr. Dwight Cavanagh, F.A.C.S., M.D., Ph.D., UTSW
   - **Title**: Professor and Vice-Chairman Dept. of Ophthalmology, UTSW
   - **Department:** Ophthalmology, UTSW **Mail Box**:
   - **Telephone**:214-648-2020, UTSW

- **Email**: Dwight.Cavanagh@UTSouthwestern.edu

4. **For a student submitting a protocol, please identify the faculty member responsible for conducting the research:**
   - **Name:** Karel J Zuzak, Ph.D., UTA
   - **Title:** Assistant Professor
   - **Department:** Bioengineering, UTA **Mail Box:**19138
   - **Telephone:** 817-272-7318 **Email:**kzuzak@uta.edu
5. **Expected Start Date:** December 1st, 2006 *(You are not authorized to start any research on human subjects until the IRB has approved the research protocol.)*
6. **Expected Completion Date:** December 1st, 2007

SECTION B: FUNDING If this research is not supported by funding, please skip to section C.

If you have or are seeking funding for your research, please specify the source.

7. **Source:** ☐ **FEDERAL (Specify Agency:)**

   ☐ **INDUSTRY SPONSORED (Specify Agency:)**

   ☐ **Local Departmental** ☐ **State** ☐ **Other:**

FUNDED GRANT / CONTRACT NUMBER:

☐ **Check here if grant is pending. Date of Grant Submission:**

8. **Do you plan to do the research if you do not receive funding?**

SECTION C: SUMMARY OF THE RESEARCH PROTOCOL

Please answer the following in simple, non-technical / non-exculpatory language.

9. **List primary research questions.** The purpose of this protocol is to develop a method to visualize the percentage of inherent blood chromophores in the retina of the eye using the non-invasive microscopic hyperspectral imaging modality. The Hyperspectral imaging method is a novel non-invasive imaging modality that uses light, to measure the percentage of inherent blood constituents. The objective of this project, is to acquire Hyperspectral Imaging data from the retina of the eye,

non-invasively and in-vivo, and calculate the percentage of inherent blood chromophores using a standard clinical eye examining slit lamp microscope.

10. **Describe the research design.** Based on the previous work of Bhavesh Shah, "In-vivo Microvasculature Visualization using Hyperspectral Imaging", where the project was successful in visualizing the vasculature of sclera of the eye, opened up the doors for potential microvasculature visualization of the retina of the eye. However the original system was modified so as to increase the sensitivity of the detector (CCD, CoolSNAPES, Princeton Instruments) and simulataneously lower the intesity of light going into the eye. This research project will be done under the supervision of Dr. Karel Zuzak, Ph.D and Dr. Dwight Cavanagh, F.A.C.S., M.D., Ph.D, of UT Arlington and UT Southwestern resplectively. The work will not begin until approval is granted by the UTA IRB. The study will consist of ten subjects. The subjects will be scheduled to visit the Laboratory of Biomedical Imaging at UTA one at a time. Once in the laboratory and after signing the consent form, the subject will be seated and relaxed for 10 minutes. The subject will be administered 3-4 pupil dilating drops, Cyclogyl ® (Alcon Laboratories Inc., Fort Worth, TX) topically and will be asked to keep the eyes close for 15 minutes. The subjects will then be asked to place their chin onto the chin rest attached to the standard clinical slit lamp, used routinely in opthalmology clinics for eye examinations. The retina of the eye will be illuminated using the light from a standard clinical slit lamp, through the diopter lens for 5 seconds while acquiring a series of digital images / pictures - Hyperspectral images. The project uses a non-invasive imaging modality, Hyperspectral Imaging, in order to determine the percentage of inherent blood chromophores in the retina. We are using a standard clinical Slit Lamp (Marco G2, Universal Opthalmic Equipment) and 78D Aspheric Diopter Lens (Volks Optical Inc.) that is typically used for standard clinical retinal examination. The filter (Liquid Crystal Tunable Filter, LCTF, Cambridge Research and Instrumentation) and the detector (CCD, CoolsnapES, Princeton Instrument) combining the hyperspectral system are integrated with the microscope to acquire a series of digital images / pictures forming a hyperspectral image cube, non-invasively and in-vivo. Briefly, the light focussed by the slit lamp through the diopter lens on the subject's retina is captured by a digital camera when it gets reflected from the subject's retina, forming a series of images, that are spectrally and statistically analysed using computer software, to determine the the percentage of inherent blood chromophores without touching the eye. The LCTF illuminates the eye with different colors of the light, which is at a lower intensity then the white light normally used in the clinic. The administration of the pupil dilating drops will be supervised by the Board Certified Opthalmologist i.e. Dr. Dwight Cavanagh.

11. **List potential benefits that may accrue to the study subjects as a result of their participation.** There are no potential benefits to the study subject.

12. **List potential benefits that may accrue to society as a result of this study.** It is hoped that the information learned from this study will help clinicians and scientists image the percentage of inherent blood chromophores non-invasively and in-vivo in the retina. The proposed research may also provide a useful method to monitor percentage of blood chromophores such as oxyhemoglobin, which is important in eye diseases such as cataract, diabetic retinopathy, glaucoma etc.

13. **What are you and your research team's relevant qualifications to perform this research? If applicable, include information about relevant licenses / medical privileges.** Nirad Zinzuwadia, MS, Principal Investigator, will be in charge of collecting the subject data, under the supervision of Dr. Zuzak, Ph.D, and Dr. Dwight Cavanagh, F.A.C.S., M.D., Ph.D. The image cubes would be acquired non-invasively and without any risk to the subjects. Dr. Zuzak developed the NIH Hyperspectral Imaging prototype, pioneered and refined the methodology for translating and utilizing this medical technology in a clinical setting. Dr. Zuzak will provide scientific expertise in the area of Hyperspectral Imaging and Dr. Cavanagh will train and supervise the Principal Investiagor in administering the right amount of drops into the subject's eye. In addition, Dr. Khosrow Behbehani, Ph.D., currently the Chair of Bioengineering at UT Arlington, will provide his expertise in digital signal processing.

14. **CHECK <u>ALL</u> RESEARCH PROCEDURES INVOLVING HUMAN SUBJECTS:**

Any materials presented to the research subject (oral or written) may not ask of the subject to provide information about another human being who has not undergone the informed consent process (this includes the immediate family of the subject).

☐ **Collection of Blood** ***State below the methods of collection (i.e. venipuncture, arterial puncture, etc.) Attach IRB Form #5 if a Tissue Repository is needed.***

☐ **Collection of Other Bodily Materials** ***State below the methods of collection. Please attach IRB Form #5 if a Tissue Repository is needed.***

☐ Analysis of Existing Data

☐ **Cognitive or Perceptual Experiment**

☐ **Evaluation of a Program or Services** ***State below whether it is Federal, State, Local, or 'Other'.***

☐ **Interview** ***State below whether it is oral or written and attach a finalized copy.***

☐ **Questionnaire or Survey** ***Attach a finalized copy***

☐ Induction of Mental or Physical Stress

☐ **Use of Private Health Information** ***State below the method for obtaining this data***

☐ Audio/Video recording of subjects

☐ **Use of Genomic DNA or Cdna**

☐ **Use of Infectious or Carcinogenic Materials**

☐ **Educational Test or Educational Materials (curriculum, books, etc.)** ***Attach copies or describe in detail***

☐ Observation of Public Behavior with PI Participation

☐ **Observation of Public Behavior without PI Participation**

☐ **Analysis of Existing Biological Specimens** ***State below where the samples were obtained from, where they will be kept and for how long, and who will have access to them.***

☐ **Deception** ***State below the debriefing procedures used***

☐ Taste Test

☒ **Medical Procedures** ***(e.g. drug, device, radiation, surgery, non-surgical manipulation, non-invasive physical measurements, etc.)***

☐ Materials Commonly Regarded as Socially Unacceptable

☐ **Use of Identified Data/Specimens**

☒ **Use of Coded Data/Specimens**

☐ **Use of Recombinant DNA** ***Attach a copy of the IBC application for Rdna along with this submission to the IRB***

☐ Use of Biohazardous Materials

☐ **Psychological Test** ***Attach Applicable copies or describe in detail***

14a. Please describe, in sufficient detail, the procedures for any checked items above. If you need more space, you may attach a separate sheet of paper.

Medical Procedures: The non-invasive digital data collected, will be used to calculate the percentage of the inherent blood chromophores. The standard clinical slit lamp source illuminates the retina of the eye through LCTF with different colors of light. The light from the LCTF is at lower intensity then the white light normally used in the clinic. Ultimately the digital camera, attached to the slit lamp using the existing C-mount on the slit lamp, captures images of the light reflected from the eye tissue, forming series of images. Spectral and statistical analysis are made using computer software, to determine the percentage of inherent blood chromophores without touching the eye surface. The administration of the pupil dilating drops will be supervised by the Board Certified Opthalmologist i.e. Dr. Dwight Cavanagh.

Use of Coded Data / Specimens: Subjects will not be identified by name in published reports or presentations of any kind. Names are removed from all specimens, forms, documents, and communications and are replaced by identifier numbers. Subject charts, test results, study casebooks, etc. are kept in the laboratory of Principle Investigator under lock and key. Digital raw data measured by the instrumentation will be identified by the corresponding identifier number and stored within a secure section of a hard drive located in the office of the Principle Investigator. Records and test results are only shared with the subject themselves or their legal parent/guardian. Confidentiality is addressed in all consent forms for the study and strictlyobserved.

14b. If the proposed research <u>is limited to</u> the use of discarded materials or retrospective chart review and there are no identifiers associating the specimens or chart information with the donors, skip sections D through G. However, if the donors can be identified, fill out section D and then skip to section H.

SECTION D: STUDY POPULATION

15. Please indicate which, if any, of the following are involved:

☐ UTA Staff

☒ UTA Faculty

☒ UTA Students

☐ **Non-English Speaking People** ***Attach the consent form and all applicable materials in the native language(s) of the subjects in the research***

☐ **Adults competent to consent for themselves (non-UTA)**

☐ **Mentally Incapacitated** ***Attach IRB Form #2A***

☐ **Children** ***(Ages 0-17 years) Attach IRB Form #2D***

☐ **Pregnant Women, Fetuses, or In Vitro Fertilization** ***Attach IRB Form#2C***

☐ **Prisoners** ***Attach IRB Form #2C***

16. Total number of subjects 10

17. Subject recruitment. Please summarize your explanation of how you will recruit subjects. Include location of recruitment and enrollment. ***Please attach a copy of all recruitment flyers and ads.*** Subjects will be recruited from the University of Texas at Arlington, by word of mouth within thecommunities at UT Arlington. Subject recruitment is one of the activities that the Principle Investigator, Nirad Zinzuwadia, MS, will over see. The subjects will be asked to follow their normal habit and will not be asked to alter from that in any way. The subjects will be volunteering to participate in this study, and they will not be compensated for their participation. Prior to collecting data, an informed consent document will be reviewed and signed by the subjects indicating that they understand and agree to voluntarily participate in the study. A standard consent form outlining the purpose of the study, procedure, risks, the benefits and compensation will be utilized. Please see attachment.

Examples of subject recruitment:

☒ **Direct person- to person solicitation per consent form.**
☐ **Telephone (attach oral presentation)**
☐ **Letter (attach finalized copy)**
☐ **Notices (attach finalized copy)**
☐ **Internet (attach finalized copy)**
☐ **Subject pool**
☐ **Other (explain and / or attach finalized copy if applicable)**

17a. List all criteria for including subjects. The study population will consist of 10 subjects between the ages of 20 to 40, that include either males or females, and not controlling for race. The experimental design aims at evaluating the percentage of inherent blood chromophores perfusing the retinal vasculature.

17b. List all criteria for excluding subjects. Subjects not fulfilling the inclusion criteria will be excluded from the study. Subjects with pulmonary or cardiac abnormalities will also be excluded. Subjects with hypertension and glaucoma will be excluded from the study as these are contraindications for the pupil dilating drops as per the manufacturers of Cyclogyl ® (Alcon Laboratories Inc., Fort Worth, TX). Additional exclusion criteria include any significant medical condition and any known eye diseases that would interfere with the conduct of the study. Also, the technique should have no impact on a fetus. However, for simplicity we will avoid imaging children (<18 years) and pregnant women. Finally, subjects unable to follow verbal commands and to cooperate with the testing will be excluded.

18. **What rewards, remuneration, or other incentives, if any, will be used to recruit subjects?** None of the subjects, will be compensated for their participation in the study.

19. **If the subject is a student who is undergoing this research for a course credit, how will you ensure that the subject was not coerced into participating?** Students will not receive course credit for participating as subjects in the study.

20. **Will you allow alternatives to the participation in the research without negative consequences?** Subjects are free to withdraw from participating in the study at any point without any consequenses.

SECTION E: CONFIDENTIALITY – PRIVACY – COERCION

21. **Does this activity utilize data collected for other purposes? (e.g. student record, student assessments, patient records, etc.) (If this is for a data**

repository, please complete and attach an IRB Form #5 as well as a Consent Form for Data Repositories)

☐**YES** ☒**NO**

a. **If yes, please specify the source of data to be utilized and how the data will be retrieved and reviewed.** Not Applicable.

b. **Could any of the recorded data contain personal or sensitive information? If yes, how do you propose to code and where will you maintain confidentiality of the data?** Subjects will not be identified by name in published reports or presentations of any kind. Names are removed from all specimens, forms, documents, and communications and are replaced by identifier numbers. Subject charts, test results, study casebooks, etc. are kept in the laboratory of Principle Investigator under lock and key. Digital raw data measured by the instrumentation will be identified by the corresponding identifier number and stored within a secure section of a hard drive located in the office of the Principle Investigator. Records and test results are only shared with the subject themselves or their legal parent / guardian. Confidentiality is addressed in all consent forms for the study and strictly observed.

(Any subject data (including documents, audio, and videotapes) developed for or used by a human subject investigation protocol are potentially sensitive and must be maintained with confidentiality. All identifiable data are to be kept in a designated locked file. Sharing of identifiable data with other institutions, agencies, or companies must be identified prospectively to both the IRB and the subjects of the study.)

22. **Could any part of this activity result in the potential identification of child abuse, elderly abuse, communicable diseases, or criminal activities that would / could not have been otherwise identified? If yes, estimate the likelihood of disclosure and describe the plan of action that you will take if this occurs.** ***In rare circumstances when research reveals these issues, confidentiality should be maintained to the extent that the law allows.***

☐**YES** ☒ **NO**

23. **Does any part of this activity have the potential for coercion of the subject? If yes, explain and describe proposed safeguards.**

☐**YES** ☒**NO**

24. **Please explain how you plan to maintain confidentiality. Include where your signed consent forms and identifiable data, if applicable, will be kept (under**

lock and key) and who will have access. Subjects will not be identified by name in published reports or presentations of any kind. Names are removed from all specimens, forms, documents, and communications and are replaced by identifier numbers. Subject charts, test results, study casebooks, etc. are kept in the laboratory of Principle Investigator under lock and key. Digital raw data measured by the instrumentation will be identified by the corresponding identifier number and stored within a secure section of a hard drive located in the office of the Principle Investigator. Records and test results are only shared with the subject themselves or their legal parent /guardian. Confidentiality is addressed in all consent forms for the study and strictly observed.

SECTION F: RISKS – PSYCHOLOGICAL RISKS

25. **Aside from possible loss of confidentiality, is there a possibility of psychological injury resulting from participating in the research?**

☐**YES** ☒**NO**

26. **If you answered yes, how do you plan to minimize and control the risks?** Not Applicable
27. **Could the desired information be obtained from animals or other laboratory models? Explain.**

☐**YES** ☒**NO**

In the event of an adverse event, you must fill out the IRB Form #8 to report the event to the Institutional Review Board for the protection of human subjects <u>immediately</u>.

SECTION G: RISKS – PHYSICAL RISKS

28. **Is there a possibility of physical injury resulting from participation in the research?**

☒**YES** ☐**NO**

29. **If you answered yes, how do you plan to minimize and control the risks?** Subjects will be asked to focus on a point and not to blink, during the 5 second data collection period, which some subjects may find inconvenient. As per the manufacturers of Cyclogyl ® (Alcon Laboratories Inc, Fort Worth, TX) the drops that are administered to dilate the pupil take about 6 to 24 hours for complete recovery of accommodation. The other discomfort / reaction may be burning, photophobia, irritation, blurred vision, irritation, hyperemia, conjunctivitis, blepharoconjunctivitis, punctuate keratitis, and synechiae as mentioned by the manufacturers of Cyclogyl ® (Alcon Laboratories Inc, Fort Worth, TX). The standard clinical slit lamp and the light source that is used in ophthalmology

clinics for routine eye examinations will be used. A Liquid Crystal Tunable Filter (LCTF) will illuminate the eye with diffirent colors of the slit lamp light that is at lower intensity than the original white light (Please refer to Appendix for further information about the source). The subjects will not be allowed to participate in the study if they have any pulmonary or cardiac abnormalities or any other serious medical condition that will interfere with the conduct of the study. Subjects with gluacoma and hypertension will also be excluded since they might have some discomfort after administering the pupil dilating drops. Female subjects that are pregnant would not be allowed to participate in the study. Further, proper instructions will be provided to the subjects once in the Laboratory, about the safety procedures they need to follow, to avoid any injuries such as, that by tripping over the equipment accidentally.

30. **Could the desired information be obtained from animals or other laboratory models? Explain.**

☐**YES** ☒ **NO**

In the event of an adverse event, you must fill out the IRB Form #8 to report the event to the Institutional Review Board for the protection of human subjects immediately.

SECTION H: COST OF RESEARCH

31. **Will the subjects incur any additional expenses for experimental (or otherwise unnecessary diagnostic) tests or procedures? If yes, explain**

☐**YES** ☒**NO**

B. **Is there any charge to the participant for participation? If yes, explain.**

☐**YES** ☒**NO**

SECTION I: INFORMED CONSENT

33. **Written, informed consent from the subject or from a legally responsible representative of the subject is normally required from the human research participants. The finalized consent form in all applicable languages should be included with the materials submitted to the IRB. You must keep all signed consent forms under lock and key during the study and for a period of 3 years after termination of the research on UTA Campus. These consent forms are subject to inspection by the Research Compliance Officer, the IRB and / or DHHS.**

If you do not plan to obtain consent or written documentation of consent, please attach a completed IRB Form # 3.

a. If appropriate, describe your rationale for obtaining oral consent or assent instead of written consent. Attach a copy of the information to be read and given to the subjects. We will provide informed consent and follow the UT Arlington policy.

b. Do you plan to make consent forms available in the native language for all subjects involved in the research? Please explain your procedures in determining the primary language spoken by the subjects and how you plan to deliver the informed consent process to subjects who do not speak English.

☐ **YES** ☒ **NO**

SECTION J: COOPERATIVE AGREEMENTS WITH OTHER INSTITUTIONS

34. If any part of this study will be conducted in an institution or location administratively separate from UTA, please indicate at which institution (attach an approval letter). Research will be conducted exclusively at UT Arlington.

b. Does this activity utilize recorded data to be sent to cooperating institutions, or agencies not under your control?

☐ **YES** ☒ **NO**

c. If yes, could the data contain personal or sensitive information or put the participant in any type of legal risk? Not Applicable

d. If yes, how do you propose to maintain the confidentiality of the data? Not Applicable.

SECTION K: CONSULTATION AND COLLABORATION

35. Subject recruitment and management:

If approval is required from other professionals for the recruitment and management of the subjects, please identify and obtain signature(s) from the individual(s) responsible for the subjects. If unobtainable, please explain or attach a signed agreement or letter.

Name of Professional	Department	Signature	Date
1.None			
2.None			
3.None			

B. **Research collaboration:**

Research collaborators are other researchers whose participation enhances the scientific merit of a research project. Have all collaborators indicate by signing this document that they have read the research protocol and agree to participate. If unobtainable, please explain or attach a signed agreement or letter.

Name of Collaborator	Department	Signature	Date
1. Karel Zuzak	BE		
2. Khosrow Behbehani	BE		
3. DwightCavanagh	Ophthalmology,UTSW		

SECTION L: CONFLICT OF INTEREST DISCLOSURE

C. **Have you submitted a financial disclosure statement to your department chair listing all of your significant financial interests in accordance with The University of Texas at Arlington conflict of interest policy?**

☒**YES** ☐**NO**

38. Did your department chair find that there was a potential conflict of interest and did he/she forward the statement to the Dean and / or the Vice President for Research and Information Technology?

☐**YES** ☒**NO**

39. If yes, please explain the conditions and restrictions imposed. If the conflict of interest is still pending review, please indicate here. Not Applicable

☐**YES** ☒ **NO**

40. Did your department chair forward the original statement to the Office of Research?

☒**YES** ☐**NO**

SECTION M: SIGNATURES

I understand that I am responsible for the accuracy of the statements made in this protocol and for the conduct of research.

I understand that I am to submit annual reviews to the Institutional Review Board for the Protection of Human Subjects. If the annual report (IRB FORM # 7) has not been received by the IRB Chair (or designee) by the anniversary date of the approval, this protocol's approval is terminated.

I understand that I am to file a final report upon conclusion of the research with the Institutional Review Board for the Protection of Human Subjects (IRB FORM # 7).

I understand that if my research is under a sponsored research agreement, additional standards may apply.

I am aware that the signed consent forms need to be filed under lock and key during the research and for a period of 3 years upon termination of the research (if unfunded). For funded research, the consent forms will be kept for the length established under the terms and conditions of the award. These consent forms will be available for inspection by the Research Compliance Officer or agents from Federal Agencies.

I understand that I, as well as all Human Subject Investigators involved in this study, must have documented Human Subject training in the Office of Research before performing any Human Subject research.

Principal Investigator **Date**

I have examined this completed form and I am satisfied with the adequacy of the proposed research design and the measures proposed for the protection of Human Subjects. I will take responsibility for informing the student of the need for safekeeping of all raw data (e.g. test protocols, tapes, questionnaires, interview notes, etc.) in a university office or computer file.

Faculty Sponsor (If not the Principal Investigator) **Date**

I have read this completed form and endorse this research to be conducted.

Department Chairman or Dean or Director **Date**

APPENDIX B

B. UTA SUBJECT CONSENT FORM

THE UNIVERSITY OF TEXAS
AT ARLINGTON

INFORMED CONSENT

PRINCIPAL INVESTIGATOR: Nirad Zinzuwadia

TITLE OF PROJECT: In-vivo Visible Reflectance Hyperspectral Imaging of Retina

This Informed Consent will explain about being a research subject in an experiment. It is important that you read this material carefully and then decide if you wish to be a volunteer.

PURPOSE

The purpose of this protocol is to develop a method to picture the blood vessels in the retina of the eye using a spectroscopic camera technically known as the hyperspectral imaging system. The camera is a novel cataract, diabetic retinopathy, glaucoma imaging system that uses light to measure the oyxgen levels in the blood. The objective of this project is to acquire series of picture using a camera and slit lamp from the retina without any pain or touch to the eye and determine the oxygenation of blood specifically the percentage of oxygenated hemoglobin in the retinal blood vessels.

DURATION

This research project is being done under the supervision of Dr. Karel Zuzak, Ph.D, and Dr. Dwight Cavanagh, F.A.C.S., M.D., Ph.D. at UT Arlington where the procedure will be carried out. The study will consist of 10 subjects. The expected duration for the study is approximately 30 minutes for a single subject.

PROCEDURES

You as a subject will be asked to visit the Laboratory of Biomedical Imaging. Once in the laboratory and after signing the consent form, you will be seated and relaxed for 10 minutes. You as a subject will then be administed 3-4 drops in the eye to dilate the pupil (Cyclogyl ®, Alcon Laboratories, Inc.is a commonly used eye drops in the ophthalmology clinics) and you will be asked to keep the eyes closed for about 15 minutes. You as a subject will then be asked to place your chin onto the chin rest attached to the standard clinical slit lamp used in eye clinics routinely used for eye examinations. A light of changing colors will be shone into your eye in order to illuminate your retina for about 5 seconds. The light intensity is not more than that used during a regular eye exam. The light that is reflected back from your retina is detected by a digital camera and saved in a computer. The computer is then used to analyze the information. There is no

contact between the instrument and your eye. We are using a standard clinical slit lamp (Marco G2, Universal Opthalmic Equipment) and a standard hand held lens that is usually used for retinal examination. The filter (Liquid Crystal Tunable Filter, LCTF, Cambridge Research and Instrumentation) and the camera (CCD, CoolsnapES, Princeton Instrument) forms the hyperspectral imaging sytem and are incorporated with the slit lamp to acquire series of digital images.

POSSIBLE RISKS / DISCOMFORTS

While the images are, being captured you, as the subject will be asked, not to blink and to focus at a point, in order to minimize eye movements that may be inconvenient to you as a subject. As per the manufacturers of drops (Alcon Laboratories Inc, TX), the drops that are administered to open up the pupil take about 6 to 24 hours for complete recovery original state. Also some of the other discomforts / reaction as per the of manufacturers of Cyclogyl ® (Alcon Laboratories, Inc., Fort Worth, TX) may be burning, excessive sensitivity to the light, irritation, blurred vision, irritation, hyperemia, and redness of the eye.

The standard clinical slit lamp has a built in light source for illuminating the eye and is used in eye clinics for routine eye examination. The light from the source is filtered to illuminate the eye with different colors of light. In addition, we have measured the intensity of the light with and without the filter and observed that the brightness is reduced with the presence of filter, which ultimately increases the safety of the eye.

Briefly, the system has a light source, very similar to a bright table lamp and a digital camera. As in a photo studio, there is a potential risk of you accidentally tripping over the equipment. Proper instructions will be given to you about the safety procedures that need to be followed during the experiment.

Otherwise, there are no potential risks (psychological, social, legal, and confidentiality) to you, as a subject of this study. However, you should not participate in the study if you have any eye disease, high blood pressure, any pulmonary or cardiac abnormalities or any other serious medical condition or history of same that will interfere with the conduct of the study. No subject should be vulnerable to this imaging technique. In addition, the technique should have no impact on a fetus. However, for simplicity we will avoid imaging children (<18 years) and pregnant women. Finally, subjects unable to follow verbal commands and to cooperate with the testing will be excluded. Also patients who are hypersensitive to eye drops (Cyclogyl ®,Alcon Laboratories, Inc.) should not participate in the study.

POSSIBLE BENEFITS

There are no potential benefits to the study subject. However, it is hoped that the information learned from this study will help eye doctors to find the oxygenation in retina noninvasively and in-vivo and monitor and detect eye disease such as cataract, diabetic

retinopathy, glaucoma at an earlier stage and help prevent blindess by inititation of treatment sooner. None of the subjects will be compensated for their participation in the study. Students will not receive course credit for participating as subjects in the study.

ALTERNATIVE PROCEDURES / TREATMENTS

You as a subject, can withdraw from participating in the study at any point without any consequenses.

CONFIDENTIALITY

Every attempt will be made to see that your study results are kept confidential. Names will be removed from all specimens, forms, documents and communication and will be replaced by identifier numbers. The Coded charts, test results, study casebooks, etc. will be kept in the Laboratory of Principle Investigator under lock and key for at least three (3) years after the end of research. Digital raw data measured by the instrumentation will be identified by the corresponding identifier number and stored within a secure section of a hard drive located in the office of the Principle Investigator. The results of this study may be published and/or presented at meetings without naming you as a subject. Although your rights and privacy will be maintained, the Secretary of the Department of Health and Human Services, the UTA IRB, the FDA (if applicable), and personnel particular to this research i.e. Nirad Zinzuwadia (Principal Investigator), Dr. Karel Zuzak (Co-Investigator and Supervising professor), Dr. Dwight Cavanagh (Co-Investigator and Supervising Professor) and Dr. Khosrow Behbehani (Co-Investigator and Bioengineering department chair) will have access to the study records. Your records will be kept completely confidential according to current legal requirements. They will not be revealed unless required by law, or as noted above.

FINANCIAL COSTS

There is no financial cost to you as a participant. You as a subject, will not be compensated for your participation in the study.

CONTACT FOR QUESTIONS

If you have any questions, problems or research-related medical problems at any time, you may call Nirad Zinzuwadia at 817-272-0809, or Dr. Karel Zuzak at 817-272-7318. You may call the Chairman of the Institutional Review Board at 817-272-1235 for any questions you may have about your rights as a research subject.

VOLUNTARY PARTICIPATION

Participation in this research experiment is voluntary. You may refuse to participate or quit at any time. You may quit by calling, Nirad Zinzuwadia, whose phone number is

817-272-0809. You will be told immediately, if any of the results of the study should reasonably be expected to make you change your mind about staying in the study. By signing below, you confirm that you have read or had this document read to you. You will be given a signed copy of this informed consent document. You have been and will continue to be given the chance to ask questions and to discuss your participation with the investigator.

You freely and voluntarily choose to be in this research project.

PRINCIPAL INVESTIGATOR: _____

DATE

_____

SIGNATURE OF VOLUNTEER **DATE**

REFERENCES

1. Lefohn A, Caruso R, Reinhard E, Budge B and Shirley Peter. An Ocularist's Approach to Human Iris Synthesis. IEEE Computer Graphics and Application. 2003; 23 (6): 70 – 75.
2. Website - http://www.nei.nih.gov/health/eyediagram/eyeimages3.asp
3. Kuivalainen A. Retinal Image Analysis Using Machine Vision. Lappeenranta University of Technology, 2005.
4. Hammer M, Thamm E and Schweitzer D. A simple algorithm for *in vivo* ocular fundus oximetry compensating for non-haemoglobin absorption and scattering. Phys. Med. Biol. 2002; 47: N233 – N238.
5. Smith MH, Denninghoff KR, Lompado A and Hillman LW. Effects of multiple light paths on retinal vessel oximetry. Applied Optics. 2000; 39 (7): 1183 – 1193.
6. de Kock JP, Tarassenko L, Glynn CJ and Hill AR. IEEE Transcations on Biomedical Engineering. 1993; 40 (8): 817 – 823.
7. Website - http://en.wikipedia.org/wiki/Hemoglobin
8. Website –

   https://sharepoint.cisat.jmu.edu/isat/klevicca/Web/isat454/hemoglobin_essay.htm
9. Shah B. Characterization of a Non-Invasive, *in vivo* Microscopic Hyperspectral Imaging System for Microvascular Visualization. University of Texas at Arlington, 2006.
10. Maltby AB. Spectrophotometric Comparison of Blood and muscle oxyhemoglobin and carboxyhemoglobin. The American Journal of Physiology, 1932.

11. Kothare A. Visible Reflectance Hyperspectral Imaging System with Improved Capabilities for Translational Medicine Projects. University of Texas at Arlington, 2005.

12. Gat N. Imaging Spectroscopy Using Tunable Filters: A Review. SPIE, 2000; 4056: 50 – 64.

13. Vo-Dinh T, Stokes DL, Wabuyele MB, Martin ME, Song JM, Jagannathan R, Michaud E, Lee RJ and Pan X. A Hyperspectral Imaging System for In Vivo Optical Diagnostics. IEEE Engineering in Medicine and Biology Society. 2004; 40 – 49.

14. Zuzak KJ, Schaeberle MD, Lewis EN and Levin IW. Visible Reflectance Hyperspectral Imaging: Characterization of a Noninvasive, In Vivo System for Determining Tissue Perfusion. Analytical Chemistry. 2002; 74 (9): 2021 – 2028.

15. Zuzak KJ, Schaeberle MD, Gladwin MT, Cannon RO III, and Lewin IW. Noninvasive determination of spatially resolved and time-resolved tissue perfusion in humans during nitric oxide inhibition and inhalation by use of a visible reflectance Hyperspectral imaging technique. Circulation, 2001; 104 (24): 2905 – 2910.

16. Eye Examination with the Slit Lamp. Carl Zeiss User Manual.

17. Meier M. The Optical Microscope (Draft). University of California Davis. 2004.

18. Website - http://www.marco.com/classical/Ultra_SL_Broch.pdf.

19. Website - http://www.cri-inc.com/products/components.asp.

20. Website - http://www.cri-inc.com/files/VariSpec_Brochure.pdf.

21. Morris HR, Hyot CC and Treado PJ. Imaging Spectrometers for Fluorescence and Raman Microscopy: Acousto-Optic and Liquid Crystal Tunable Filters. Applied Optics. 1994; 48: 857 – 866.

22. Poger S and Angelopoulou E. Selecting components for building multispectral sensors. IEEE CVPR technical sketches (CVPR Tech Sketches). IEEE Press, New York. 2001.

23. Slwason RW, Ninkov Z and Horch E. Hyperspectral Imaging: Wide-Area Spectrophotometry Using a Liquid-Crystal Tunable Filter. Publication of the Astronomical Society of the Pacific,1999; 111: 621 – 626.

24. Miller PJ. Use of Tunable Liquid Crystal Filters to Link Radiometric and Photometric Standards. Metrologia, 1991; 28: 145 – 149.

25. VariSpec ™ Liquid Crystal Tunable Filter User's Manual, Cabridge Research and Instrumentation.

26. SBIG Astronomical Instruments Manual, Santa Barbara Instrument Group.

27. PIXIS System User Manual, Princenton Instruments.

28. The Basics of Camera Technology, Technical Manual, SONY.

29. CoolSNAP Interline Camera, Roper Scientific Inc..

    (Source: http://www.piacton.com/pdfs/whitepapers/interline.pdf)

30. Leal MJ. Effect of Pixel Size and Scintillator on Image Quality of a CCD-Based Digital X-ray Imaging System. Worcester Polytechnic Institute, 2001.

31. Website - http://www.photomet.com/software/software_pvcam.php.

32. Getting Started with V++, User manual, Digital Optics Ltd.

33. Website - http://volk.com/classic-78d.aspx.

34. Zuzak KJ, Naik SC, Alexandrakis G, Hawkins DM, Behbehani K and Livingston EH. Characterization of a Near-Infrared Laparoscopic Hyperspectral Imaging System for Minimally Invasive Surgery. Analytical Chemistry, 2007; 79 (12): 4709 – 4715.

35. Press WH, Flannery BP, Teukoslky SA, Vetterling WT. Numerical Recipes in C: The Art of Scientific Computing. NY: Cambridge University Press, 1992.

36. Website - http://www.dscp.dla.mil/GI/general/lightcat/Cookecal.pdf

37. Website - http://www.efg2.com/Lab/ImageProcessing/TestTargets/Image133.gif

38. Website - http://en.wikipedia.org/wiki/Spectralon

39. Moller W, Nilolaus KP and Hope A. Degradation of the diffuse reflectance of Spectralon under low-level irradiation. Metrologia, 2003; 40: S212 – S215.

40. Springer Series. Verbeke G and Molenberghs G. Linear Mixed Models for Longitudinal Data. Springer, 2000.

BIOGRAPHICAL INFORMATION

Nirad Zinzuwadia was born on 18th January, 1983 in Vadodara, Gujarat, India. He completed his Bachelor of Engineering in Biomedical Engineering from Saurashtra University, India in June 2004. He then worked as a Biomedical Engineer for 6 months after which he joined University of Texas at Arlington in Fall 2005 to pursue Masters of Science in Biomedical Engineering. His current research area is hyperspectral imaging. Apart from hyperspectral imaging, his research areas of interest is Bioinstrumentation and Medical Imaging especially CT and MRI.